

FINAL REPORT

**ROCK SCOUR ANALYSIS
FOR THE
I-10 BRIDGE CROSSING OF THE CHIPOLA RIVER
BRIDGE NO. 530052 (WESTBOUND)
BRIDGE NO. 530053 (EASTBOUND)**

SUBMITTED TO:

**E.C. DRIVER AND ASSOCIATES, INC.
7119 BEACH RIDGE TRAIL
TALLAHASSEE, FLORIDA 32312-5075**

AND

**FLORIDA DEPARTMENT OF TRANSPORTATION
DISTRICT 3
CHIPLEY, FLORIDA**

SUBMITTED BY:

**OEA, INC.
5329 NW 33RD PLACE
GAINESVILLE, FLORIDA 32606**

DECEMBER 2001

EXECUTIVE SUMMARY

The sediments at the I-10 Chipola River Bridge site in Jackson County, Florida are predominately lime rock. However, this material does not meet the Federal Highway Administration's criteria for a nonerodible sediment and thus must be treated as a cohesionless sediment (sand) for estimating bridge scour depths unless further tests show otherwise. The purpose of this study was to determine the rate-of-erosion properties of this material due to shear stresses created by water flow (simulating shear stresses created by river discharge). This was accomplished by testing core samples at the elevation of the existing channel bed by an apparatus developed at the University of Florida in Gainesville, Florida. Estimates of total (contraction plus local) scour depths at the channel piers were then made, at five year intervals for the anticipated life of the structure, based on the test results and a very conservative projected fifty year flow discharge hydrograph. All of the rock samples were found to be scour resistant for the range of anticipated shear stresses. The maximum scour depth at the end of fifty years is estimated to be approximately 0.04 ft (0.5 in).

ROCK SCOUR ANALYSIS FOR THE I-10 BRIDGE CROSSING OF THE CHIPOLA RIVER

Introduction:

Erodable rock is found at a number of bridge sites throughout the State of Florida. The composition of these softer rock materials is one or more of the following: limerock, consolidated sandstone, coquina or coral. Often the geotechnical properties of the rock materials are not sufficient for it to be considered as “unscourable” by the Federal Highway Administration (FHWA) as described in their Hydraulic Engineering Circular No. 18 (HEC-18) and thus are considered as cohesionless sediments for the purpose of estimating design bridge scour depths. In many cases this yields overly conservative design scour depths that translate into excessive costs in the construction of new bridges or in the retrofitting of existing bridges. The Florida Department of Transportation (FDOT) State Drainage Engineer’s Office has recommended that when the FDOT Districts encounter these materials a special investigation that includes the State Drainage Office be made to determine the appropriate design scour depths for that site. It is recognized that there is significant variability from one site to the next and that if improved scour estimates are to be made each case must be considered individually. As part of this investigation the State Drainage Engineer’s Office has recommended that cores from the site be tested for “Rate of Erosion” characteristics. These tests provide information on the rate at which these materials will erode as a function of the intensity of the water flow over them. The results of these tests are presented as plots of Rate of Erosion versus Bed Shear Stress. For fully developed water flow the depth averaged velocity can be related to the bed shear stress. By formulating a conservative water flow hydrograph for the expected life of the structure an estimate of the ultimate scour depth at the structure can be made. However, this information is but one of a number of parameters that must be considered in arriving at appropriate design scour depths for the structure. Other parameters to be considered include the nature and thickness of the rock strata; is the rock directly exposed to the flow or is it beneath other sediments; did fracturing of the rock occur (or will fracturing occur) during construction of the bridge, if the rock is fractured, how far out from the structure(s) does this extend and what is the range of sizes of the rock fragments; for existing bridges what extreme flow events has the bridge experienced and what if any (contraction, local) scour has been observed? Once the information needed to answer these questions has been compiled and analyzed, more accurate estimates of design scour depths can be made.

Scope of this Investigation:

The objective of this investigation was to produce more accurate estimates of bridge scour depths likely to be encountered at the I-10 crossing of the Chipola River in Jackson County, Florida during its lifetime. To achieve this objective the following tasks were to be performed:

1. Compile information on the bridge piers, freshwater discharge, historical scour issues and sediments (geotechnical core information).
2. Review core samples taken at the site. Obtain appropriate core samples for Rate of Erosion tests.
2. Conduct a site visit to obtain first hand information about existing conditions.
3. Analyze data obtained in 1) and 2) to determine if existing information is sufficient for the analyses.
4. Prepare core samples and conduct Rate of Erosion tests at the University of Florida.
5. Reduce and analyze Rate of Erosion data.
6. Generate a conservative hydrograph for the remainder of the life of the existing bridges.
7. Based on the rate of erosion data and the projected hydrograph, produce a conservative estimate of the maximum scour depths at two of the existing piers on each of the two bridges at the site.

Approach Taken and Basis for Analysis:

When rock is encountered at a bridge site, samples of the rock must be analyzed to determine if it is to be considered erodable. The FHWA in their HEC-18 (2001) has established a criterion for erodability. The most recent edition of HEC-18 (Fourth Edition) was published in May 2001. Until recently once a rock was classified as erodable it was treated as a cohesionless sediment (sand). In some cases this resulted in gross over-predictions of design scour depths. With the development of apparatus for measuring rate of erosion as a function of applied shear stress, better estimates of design scour depths can be obtained. The University of Florida has developed two such apparatus, one is a recirculating flume patterned after one developed by Professor Wilber Lick at the University of California at Santa Barbara, California. Professor Jean-Luis Briaud at Texas A&M University has a similar apparatus that is used for measuring the rate of erosion in cohesive sediments. The University of Florida apparatus is under construction and should be operational during the first quarter of 2002.

The University of Florida has also developed a second apparatus for measuring rate of erosion. This apparatus, which was used for this analysis, has been operational for approximately two years and is limited to testing sediments that can support their own weight. That is, more rigid sediments that will not deform under their own weight. The apparatus [referred to here as the Rotating Erosion Test Apparatus (RETA)] is shown in Figures 1 and 2. A technical paper on the initial version of this apparatus was presented at the International Symposium on Scour at Foundations Melbourne, Australia on

November 19, 2000 [Henderson, et al. (2000)]. A copy of this paper is included in Appendix A of this report.



Figure 1. Photograph of Rotating Erosion Test Apparatus (RETA).



Figure 2. Close-up of RETA.

An improved version of the apparatus described in the paper was used to measure the rate of erosion of the core samples from the I-10 Chipola River Bridge site.

In the case of erodable rock there are additional conditions that must be met prior to using these types of apparatus. For the rates of erosion obtained from these apparatus to apply to the rock at the site of interest, it must be such that it erodes and is not transported as rock fragments. The rock must be a continuous stratum or layer. Also, if the rock stratum is fragmented, the size of the fragments must be such that they will not be transported by the design flows. Knowledge of the type and condition of the rock formation can be obtained by a site inspection and examination of the boring logs. In general, the site inspection will require the use of divers to inspect the bed near the piers for existing bridges. For proposed bridges knowledge of the pier design and construction techniques to be used are needed when estimating the condition of the rock bed. If the rock bed is highly fractured (i.e. the rock fragments are likely to be transported by the design flows) then a technique such as that proposed by Annandale (1995) should be used to estimate scour depths. The rock at the I-10 Chipola River Bridge site meets the criterion for using the rate of erosion approach.

Once it has been established that the rock bed is continuous, that the fractured rock segments are of sufficient size that they will not be moved by the flows to be encountered, the RETA can be used to determine the rate of erosion properties of the sediment. The rate of erosion versus bed shear stress relationships obtained from the laboratory tests can be used to estimate both contraction and local scour depths for the projected structure life hydrograph. The procedure for estimating scour depths consists of the following steps:

1. Establish a hydrograph of depth averaged velocity and water depth for the time interval of interest.
2. Establish the relationship between depth averaged velocity and bed shear stress.
3. Obtain rate of erosion versus bed shear stress information from laboratory testing of core samples from the site.
4. Knowing the erosion rate as a function of bed shear stress and the bed shear stress as a function of time the product of these two will yield the scour depth as a function of time:

$$\text{Scour Depth (ft)} = \left[\text{Rate of Erosion} \left(\frac{\text{ft/hr}}{\text{lb}_f / \text{ft}^2} \right) \right] \left[\text{Bed Shear Stress} \left(\text{lb}_f / \text{ft}^2 \right) \right] \left[\text{Duration (hr)} \right]$$

Contraction scour estimates are straightforward as the bed shear stress for these conditions is easier to estimate as a function of the depth averaged velocity in the stream. On the other hand the shear stresses that produce local scour are more complex and difficult to estimate. It is known that the maximum shear stress in a scour hole varies with scour hole depth from some initial value to the (sediment) critical value when the equilibrium depth has been reached. This variation is depicted in the sketch shown in Figure 3.

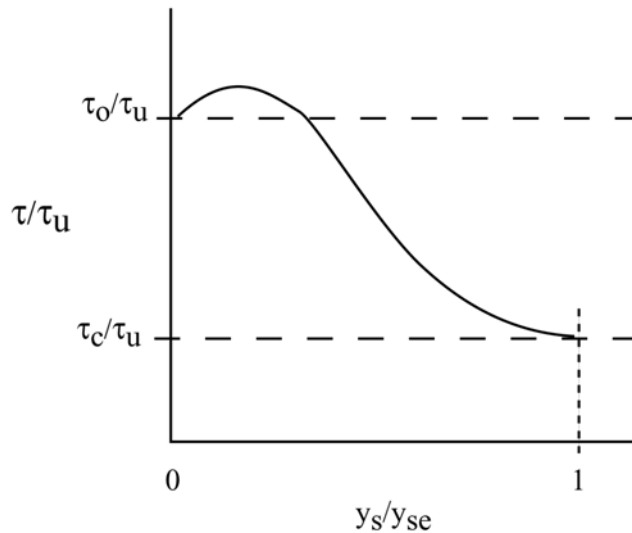


Figure 3. Sketch showing maximum effective bed shear stress in a scour hole at a circular pile in a steady flow. τ_u is the bed shear stress just upstream of the pier, τ_0 is the maximum shear stress at the pier prior to scour, τ_c is the sediment critical shear stress and y_s and y_{se} are the instantaneous and equilibrium local scour depths respectively.

Figure 3 shows the general relationship between the maximum shear stress in the scour hole as a function of 1) the upstream bed shear stress, 2) equilibrium scour depth and 3) the depth of the instantaneous scour hole depth. This relationship was established for local scour holes in cohesionless sediments at a single circular pile. Investigations of local scour hole shapes in rock sediments have not been reported in the open literature but they will most likely be different than those for cohesionless sediments and thus, the shear stress versus scour depth will be different. For design purposes it is sufficient to assume that the maximum shear stress at the structure remains a multiple of the upstream shear stress throughout the scour process. A conservative but reasonable assumption is that the ratio of shear stress at the structure to the upstream bed is constant and equal to the initial (pre-scour) value. For circular piles this ratio has been shown to be approximately 5.0. For square piles this value is estimated to be about 15% larger. In this analysis the conservative ratio of 6.0 was used for estimating local scour depths at the square pile piers.

Existing Data/Information:

Bridge piers considered in this analysis:

Figures 4 and 5 show the location of the bridges under consideration. There are two bridges at this site, one for the eastbound traffic (Bridge No. 530053R) and one for the westbound traffic (Bridge No. 530052L). Photographs of the two bridges are shown in Figures 6 and 7. Piers 4 and 5 for both bridges are being analyzed as part of this study.

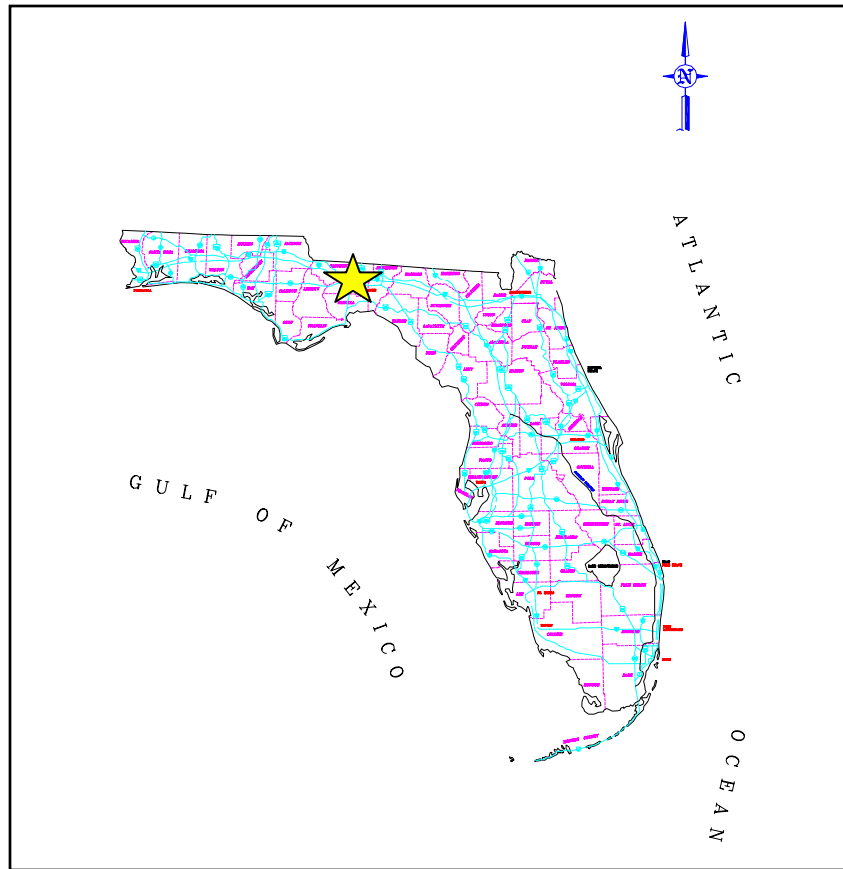


Figure 4. Location map for the I-10 Chipola River Bridges (Jackson County, Florida).

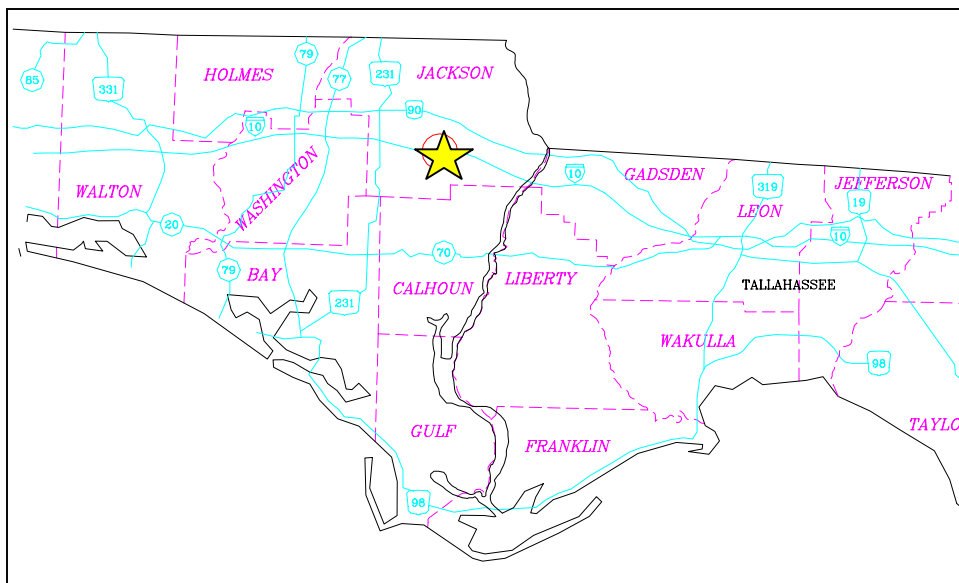


Figure 5. More detailed location map for the I-10 Chipola River Bridges.

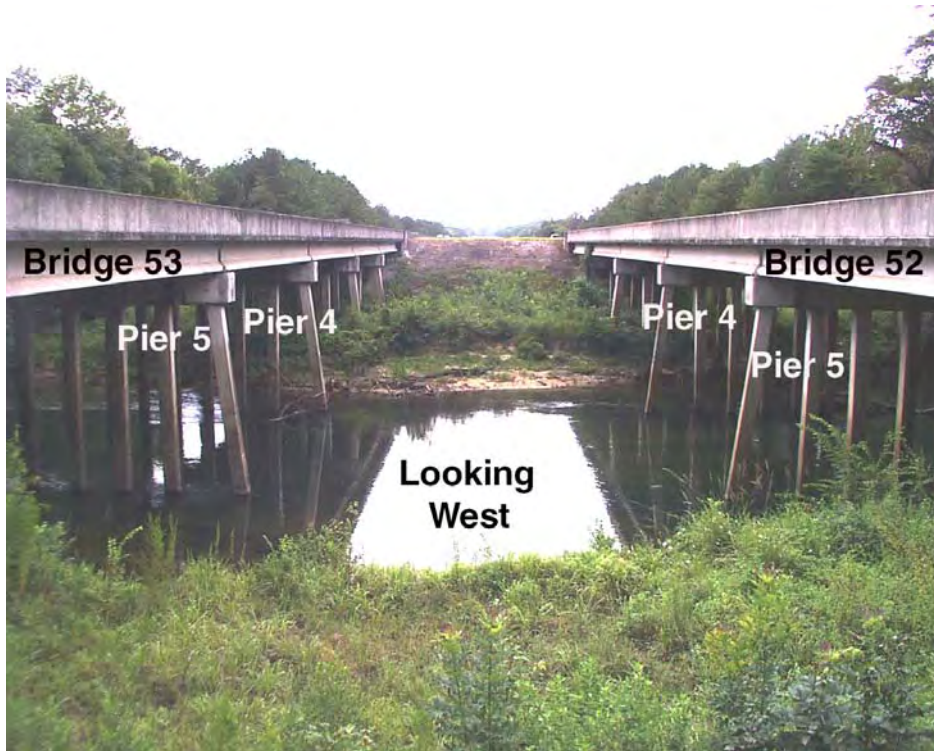


Figure 6. Bridges 52 and 53 Looking West

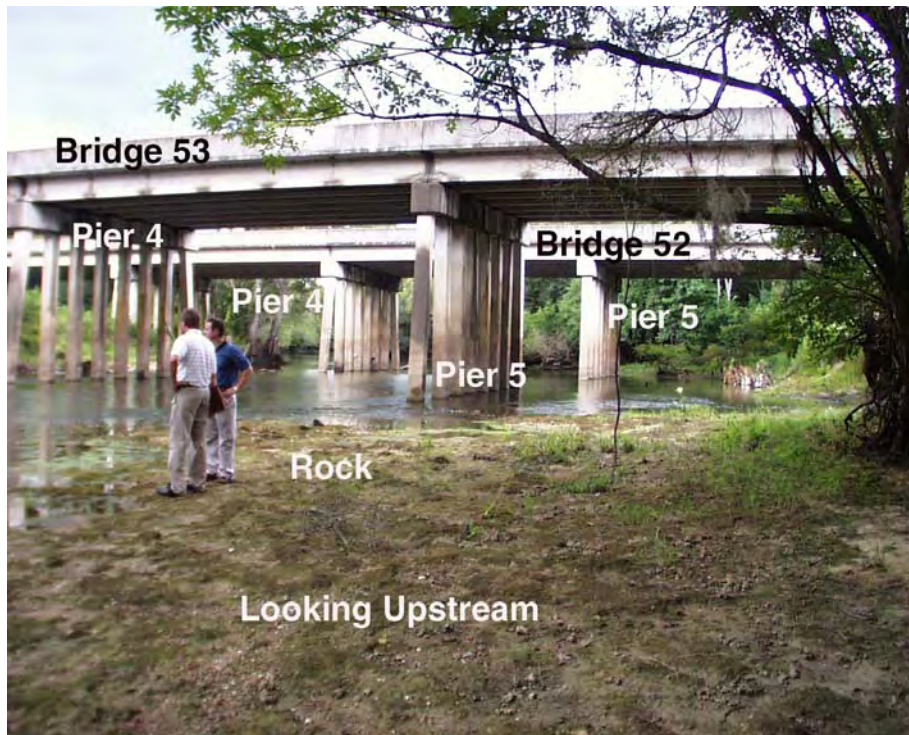


Figure 7. Bridges 52 and 53 Looking Upstream 2

Figures 8 and 9 are plan views of the bridges showing the four borehole locations used in this study. These figures were taken from two geotechnical reports by Ardaman and Associates, Inc. (1998). Figures 10 and 11 are drawings of Piers 4 and 5 on the westbound bridge (No. 530052L) and eastbound bridge (No. 530053R) respectively. These figures were taken from the Phase II scour analysis report by David Volkert and Associates, Inc. (1998). The piers consist of 1 x 8 pile groups (one pile normal to the flow and eight in-line with the flow). The end piles are battered in the direction of the stream. The piles are 1.5-ft wide square piles with a centerline spacing of 4.5 ft. The pile cap is normally out of the water but according to the hydraulic analysis performed by David Volkert and Associates, Inc. (1998), is submerged during 100- and 500-year design storm events. According to their hydraulic analysis the piers are aligned with the flow so that there is no flow skew angle during the 100- and 500-year design storm events.

Summary of hydrologic and hydraulic information:

The hydraulic analysis and scour computations were performed by David Volkert and Associates, Inc. A summary of the hydrologic, hydraulic, and scour data/information for the site is presented in Tables 1 - 3 along with the sources of the information.

Table 1. Design storm discharges¹.

Computed Drainage and Discharge	
Drainage Area	587.2 (sq. miles)
2-YR Discharge Q ₂ ²	4962.1 CFS
10-YR Discharge Q ₁₀ ²	10,196.6 CFS
25-YR Discharge Q ₂₅ ²	13,629.1 CFS
50-YR Discharge Q ₅₀ ²	16,605.5 CFS
100-YR Discharge Q ₁₀₀ ²	19,742.3 CFS
500-YR Discharge Q ₅₀₀ ²	28,407.7 CFS

Table 2. Hydraulic data used for contraction scour computations¹.

Contraction Scour		
	100 Year	500 Year
Channel Average Velocity	4.24 ft/s	4.46 ft/s

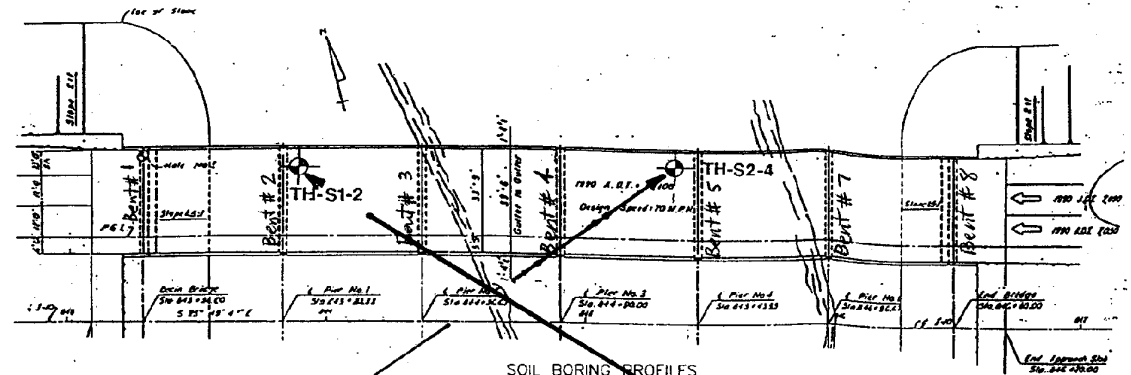
Table 3. Hydraulic data used for local scour computations¹.

Local Scour		
Hydraulic Data	100 Year	500 Year
Westbound Bridge (No. 530052L)		
Upstream Velocity (Piers 4 and 5)	7.38 ft/s	9.36 ft/s
Eastbound Bridge (No. 530053R)		
Upstream Velocity (Piers 4 and 5)	7.08 ft/s	9.11 ft/s

¹ Source-Scour Evaluation Report, David Volkert and Associates, Inc.

² USGS Regression Equations

NOTE: PILE TIP ELEVATIONS SHOWN ARE FOR THE CONCRETE PORTION OF THE PILE 'TIPS' AT 6 FEET ABOVE THE STEEL STINGER TIP.



LEGEND

TH STANDARD PENETRATION TEST (SPT) BORING LOCATION
 IN STANDARD PENETRATION RESISTANCE IN BLOWS PER FOOT
 CASHING
 --- AVE. EXISTING GROUND LINE (---)
 --- AVE. 100 YEAR SCOUR LINE (---)
 --- AVE. PILE TIP ELEVATION (---)
 [---] BASED ON DAVID VOLKERT & ASSOCIATES, INC.
 SPT, SU UNIFIED SOIL CLASSIFICATION SYSTEM
 ROCK CORING DATA
 R RECOVERY (RO)
 CORE SIZE = 1/4" DIA
 STANDARD PENETRATION TEST DATA
 SPOON I.D. = 1.317" HANMER DROP = 30"
 SPOON O.D. = 2.0" HANMER WEIGHT = 140 lbs.

ENGINEERING CLASSIFICATION

I COHESIONLESS SOILS

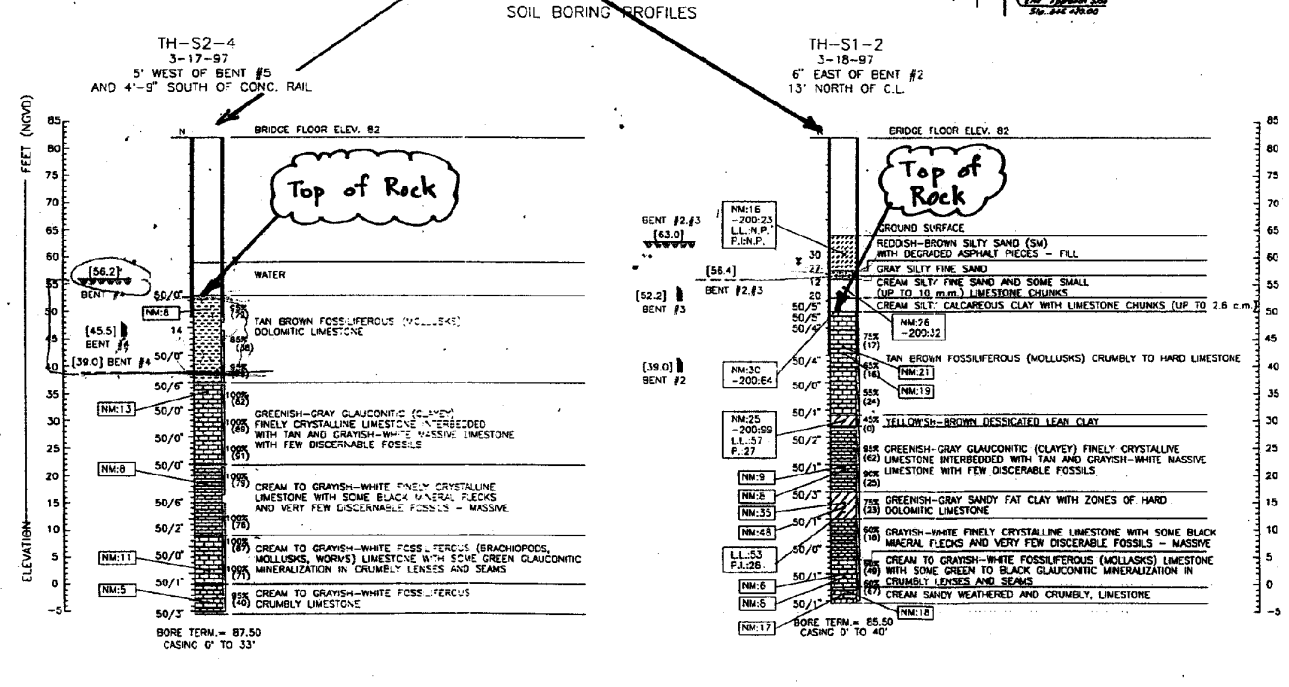
DESCRIPTION	BLOW COUNT "N"
VERY LOOSE	0 TO 4
LOOSE	4 TO 10
MEDIUM	10 TO 30
DENSE	30 TO 50
VERY DENSE	>50

II COHESIVE SOILS

DESCRIPTION	UNCONFIRMED COMPRESSIVE STRENGTH, QIL TSP	BLOW COUNT "N"
VERY SOFT	<1/4	0 TO 4
SOFT	1/4 TO 1/2	4 TO 10
MEDIUM	1/2 TO 1	10 TO 30
STIFF	1 TO 2	30 TO 50
VERY STIFF	2 TO 4	15 TO 30
HARD	>4	>50

WHILE THE BORINGS ARE REPRESENTATIVE OF SUBSURFACE CONDITIONS AT THEIR RESPECTIVE LOCATIONS AND FOR THEIR RESPECTIVE VERTICAL REACHES, LOCAL VARIATIONS CHARACTERISTIC OF THE SUBSURFACE MATERIALS OF THE REGION ARE ANTICIPATED AND MAY BE ENCOUNTERED. THE BORING LOGS AND RELATED INFORMATION ARE BASED ON THE DRILLER'S LOGS AND VISUAL EXAMINATION OF SELECTED SAMPLES IN THE LABORATORY. THE DELINEATION BETWEEN SOIL TYPES SHOWN ON THE LOGS IS APPROXIMATE AND THE DESCRIPTION REPRESENTS OUR INTERPRETATION OF SUBSURFACE CONDITIONS AT THE DESIGNATED BORING LOCATIONS ON THE PARTICULAR DATE DRILLED.

GROUNDWATER AND SURFACE WATER ELEVATIONS SHOWN ON THE BORING LOGS REPRESENT GROUNDWATER AND SURFACE WATER SURFACES ENCOUNTERED ON THE DATES SHOWN. FLUCTUATIONS IN WATER LEVELS SHOULD BE ANTICIPATED THROUGHOUT THE YEAR.



REVISIONS				DATE		BY		REVISIONS		DATE		BY	
ENGINEER OF RECORD: STEPHEN P. SHANKLY, P.E. FL REG. NO. 46663 Ardaman & Associates, Inc. 3175 W. THURMAYE STREET TALLAHASSEE, FL 32302 (904) 576-6137				LOGG: Ardaman & Associates, Inc.		SEAL: 		FLORIDA DEPARTMENT OF TRANSPORTATION GEOTECHNICAL DESIGN OFFICE		SHEET TITLE: REPORT OF CORE BORINGS		Drawing No.: FIGURE 1	
REVISIONS Drawn by: SPB 5/97 Checked by: SPB 5/97 Designed by: SPB 5/97 Drawn by: SPB 5/97 Approved by: STEPHEN P. SHANKLY, P.E.				PROJECT NO.: BRIDGE # 530052L S.R. 8 OVER CHIPOLA RIVER JACKSON COUNTY, FLORIDA		PROJECT NO.: 99906-1528		PROJECT NO.: BRIDGE # 530052L S.R. 8 OVER CHIPOLA RIVER JACKSON COUNTY, FLORIDA		Drawn No.: FIGURE 1		Scale No.: 	

Figure 8. Boring log for boreholes S1-2 and S2-4 under westbound Bridge No. 530052.

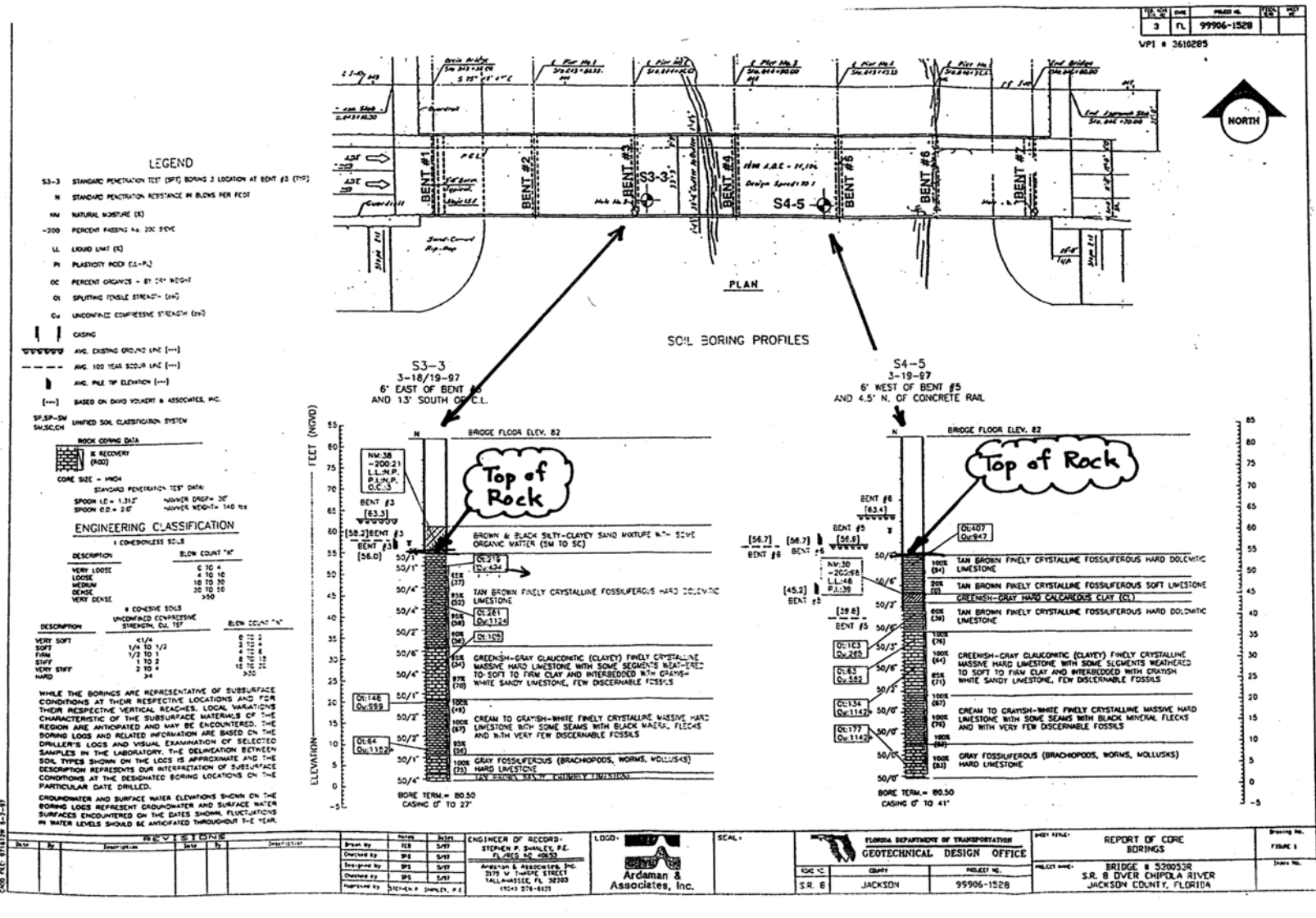


Figure 9. Boring log for boreholes S3-3 and S4-5 under eastbound Bridge No. 530053R.

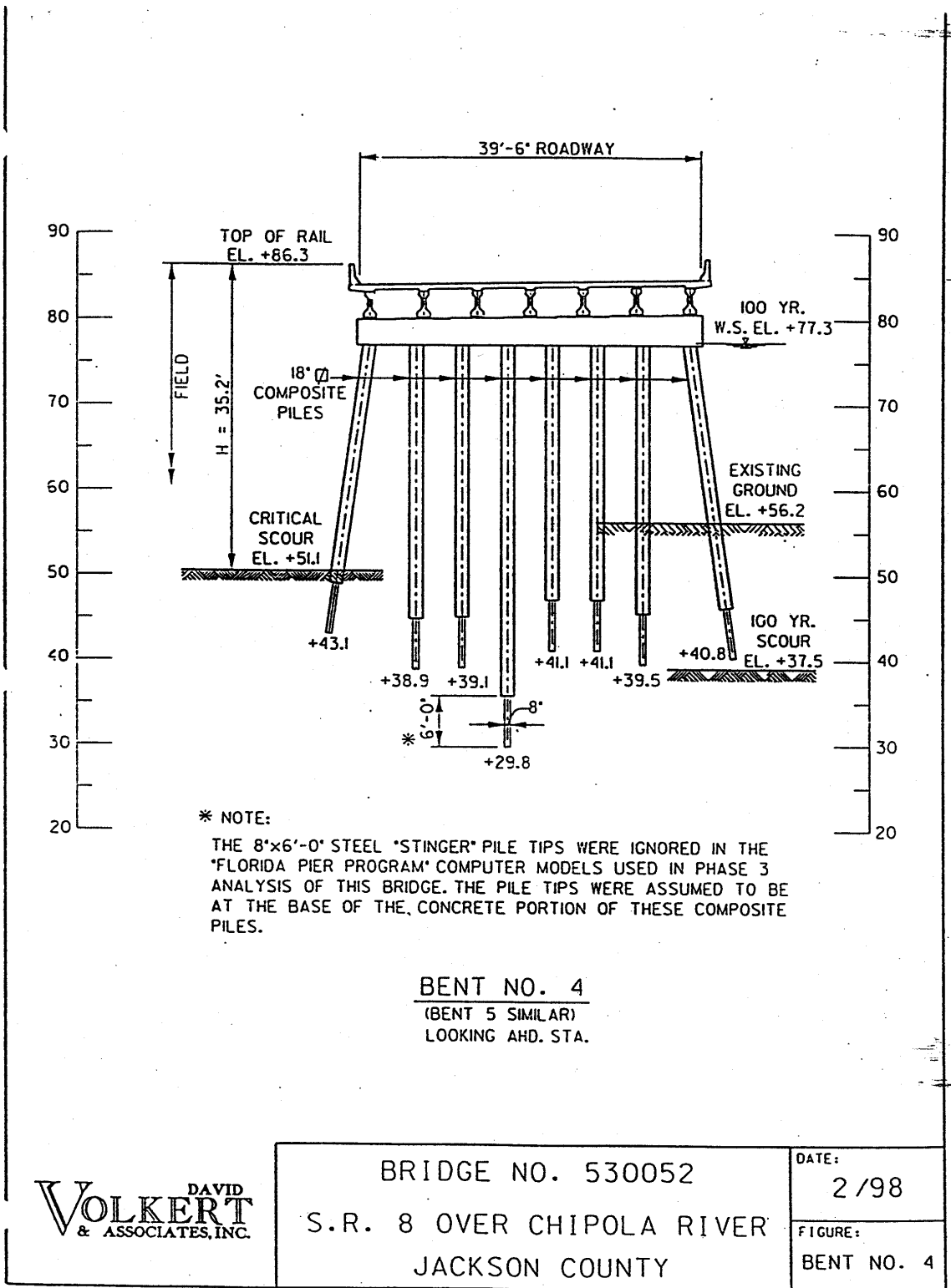


Figure 10. Piers 4 and 5 on Bridge No. 530052

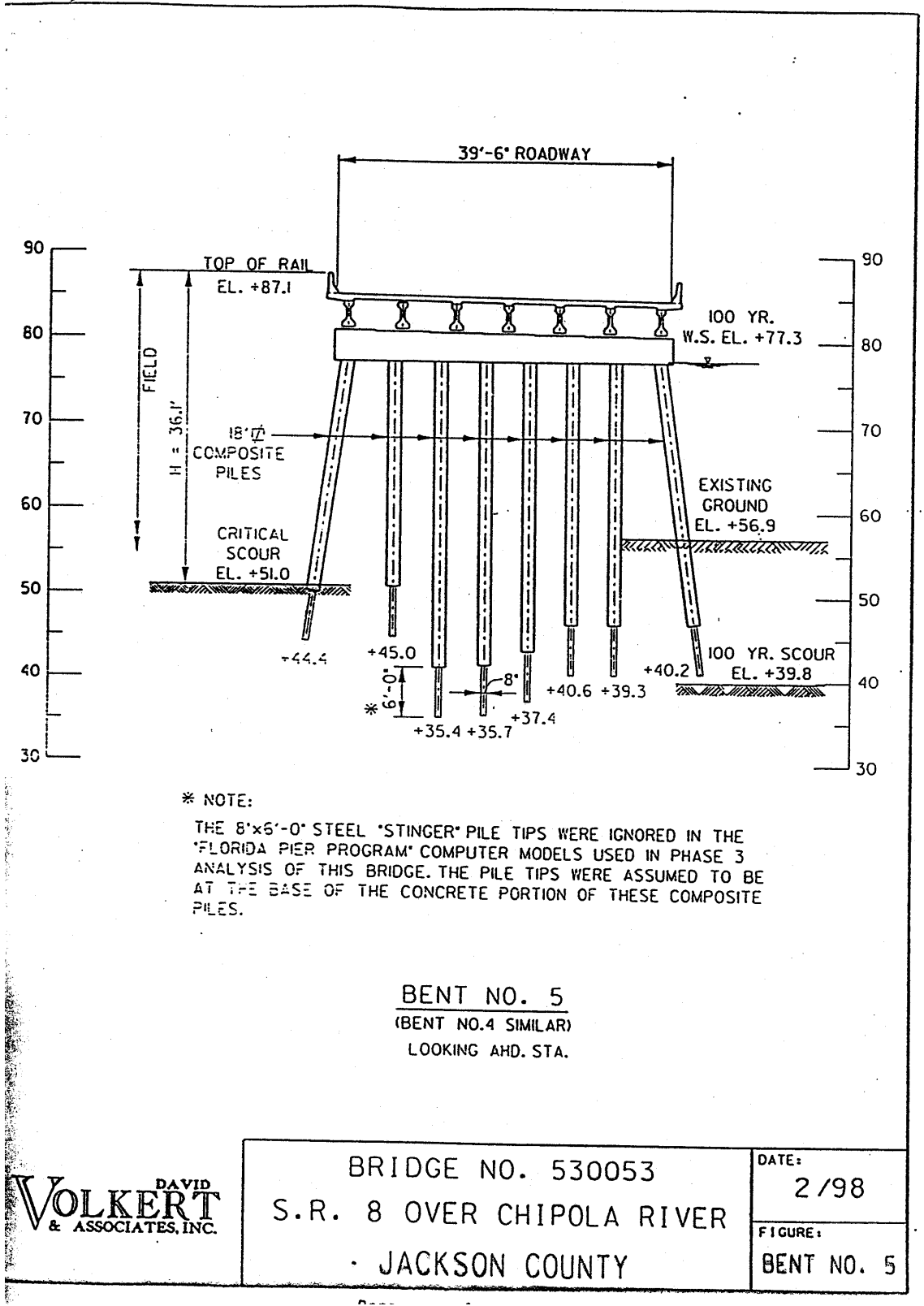


Figure 11. Piers 4 and 5 on Bridge No. 530053.

Historical flow discharge data:

The USGS has collected discharge data for the Chipola River at Gauge Number 02359000 for many years. The location of this gauge is shown in Figures 12 and 13. The gauge is approximately 12 miles downstream of the I-10 Chipola River Bridge.

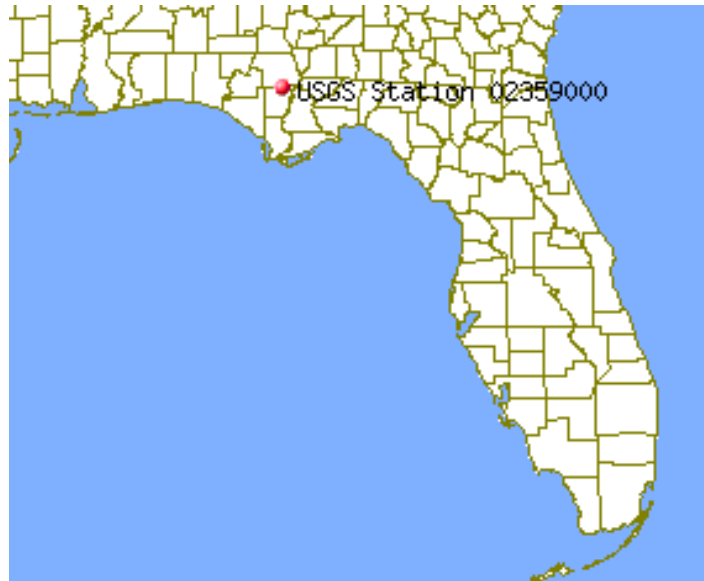


Figure 12. Location map for USGS Gauge No. 02359000.

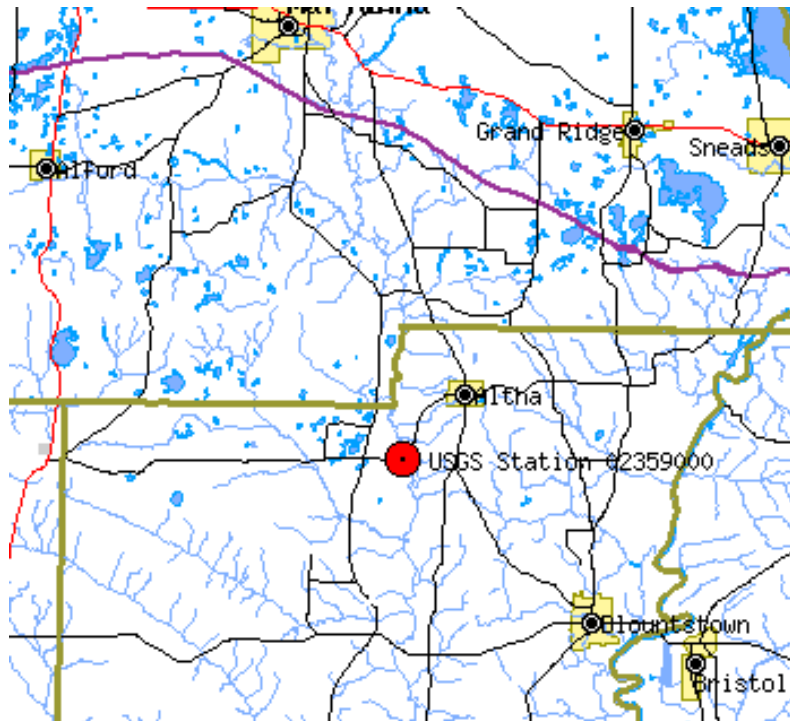


Figure 13. More detailed location map for USGS Gauge No. 02359000

Discharge data from this gauge includes discharge at the I-10 Bridge plus runoff from the portion of the drainage basin between I-10 and the gauge. The drainage basin at the gauge is 781 mi² as compared to 587 mi² at the I-10 Bridge site. Use of data from this gauge for the I-10 Bridge will therefore be conservative (discharges will be larger than the actual values at the I-10 Bridge). The data presented in Figure 14 and Table 4 are the yearly maximum discharges and water elevations at the gauge from 1913 to 2000. Daily discharges from this gauge are given in a Microsoft EXCEL file on the attached CD. Plots of Flow discharge versus water depth for two different time periods are given in Figures 15 and 16. Note that there is a significant difference in the relationship between discharge and depth for the two intervals. Information from this gauge was used to establish the discharge hydrographs for the rock scour analysis.

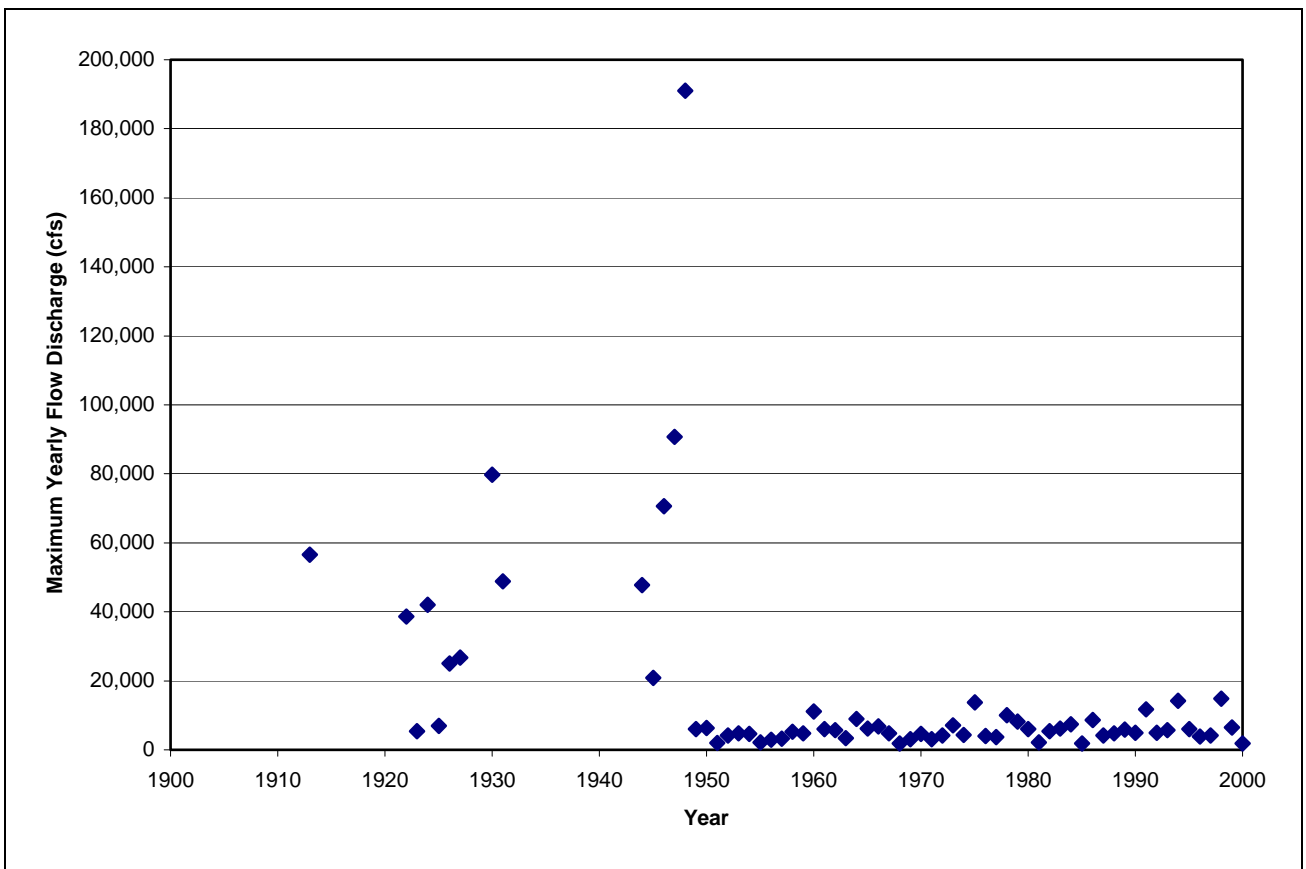


Figure 14. Maximum yearly flow discharges at USGS Gauge No. 02359000 on the Chipola River.

Table 4. Yearly maximums of flow discharge and water elevation at USGS Gauge No. 02359000 on the Chipola River from 1913-2000 (with some gaps).

Year	Date	Gauge Height (feet)	Stream-flow (cfs)	Year	Date	Gage Height (feet)	Stream-flow (cfs)
1913	Mar. 22, 1913	21.1	56,501	1968	Jan. 2, 1968	11.42	1,830
1922	Jun. 2, 1922	15.98	38,701	1969	Sep. 21, 1969	14.83	3,100
1923	Jun. 29, 1923	20.7	5,460	1970	Feb. 18, 1970	18.93	4,630
1924	Sep. 16, 1924	17.6	42,001	1971	Mar. 20, 1971	14.68	3,040
1925	Jan. 24, 1925	23.7	7,010	1972	Jun. 27, 1972	17.67	4,240
1926	Sep. 20, 1926	33.55	25,000	1973	Apr. 5, 1973	23.42	7,070
1927	Nov. 22, 1926	13.52	26,801	1974	Feb. 13, 1974	18.05	4,390
1930	Oct. 2, 1929	25.2	79,801	1975	Apr. 16, 1975	29.43	13,800
1931	Nov. 22, 1930	19.44	48,801	1976	Feb. 1, 1976	17.11	4,040
1944	Mar. 28, 1944	19.18	47,801	1977	Dec. 4, 1976	16.29	3,650
1945	Feb. 12, 1945	12.33	20,901	1978	Mar. 14, 1978	26.98	9,980
1946	May 22, 1946	23.85	70,701	1979	Mar. 2, 1979	25.09	8,210
1947	Mar. 13, 1947	26.42	90,801	1980	Mar. 18, 1980	21.91	6,060
1948	Apr. 4, 1948	32.2	191,001	1981	Feb. 11, 1981	12.03	2,120
1949	Dec. 13, 1948	21.95	6,100	1982	Feb. 8, 1982	19.81	5,340
1950	Sep. 1, 1950	22.5	6,350	1983	Apr. 16, 1983	22.13	6,170
1951	Apr. 4, 1951	11.88	1,940	1984	Mar. 7, 1984	24.52	7,380
1952	Feb. 21, 1952	17.93	4,180	1985	Feb. 11, 1985	11.33	1,850
1953	Apr. 13, 1953	19.12	4,720	1986	Feb. 12, 1986	26.05	8,710
1954	Dec. 28, 1953	18.9	4,620	1987	Mar. 6, 1987	17.83	4,170
1955	May 28, 1955	12.56	2,220	1988	Mar. 10, 1988	19.69	4,840
1956	Jul. 4, 1956	14.53	2,900	1989	Jun. 14, 1989	21.75	5,860
1957	Jun. 9, 1957	15.55	3,270	1990	Jan. 14, 1990		5,000
1958	Apr. 16, 1958	20.38	5,310	1991	Mar. 4, 1991		11,800
1959	Apr. 3, 1959	19.11	4,720	1992	Mar. 11, 1992	20.17	4,950
1960	Apr. 8, 1960	28.42	11,100	1993	Jan. 17, 1993	22.07	5,790
1961	Apr. 21, 1961	21.96	6,080	1994	Jul. 11, 1994	29.60	14,200
1962	Apr. 6, 1962	21.25	5,720	1995	Oct. 3, 1994	22.59	6,020
1963	Jul. 27, 1963	15.81	3,360	1996	Apr. 1, 1996	17.28	3,860
1964	May 7, 1964	26.05	8,960	1997	Jan. 14, 1997	18.07	4,170
1965	Dec. 31, 1964	21.85	6,180	1998	Mar. 13, 1998	30.73	14,800
1966	Mar. 6, 1966	22.85	6,730	1999	Oct. 1, 1998	22.95	6,470
1967	Jan. 11, 1967	19.03	4,810	2000	Feb. 15, 2000	11.82	1,920

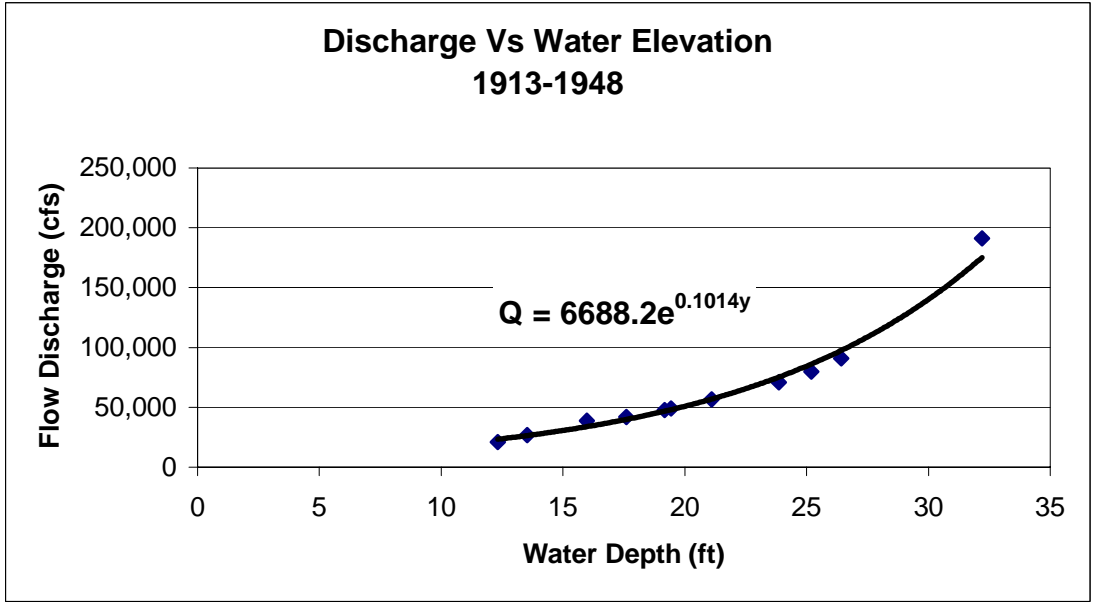


Figure 15. Flow discharge versus water elevation from 1913-1948 (excluding 3 years of reported data).

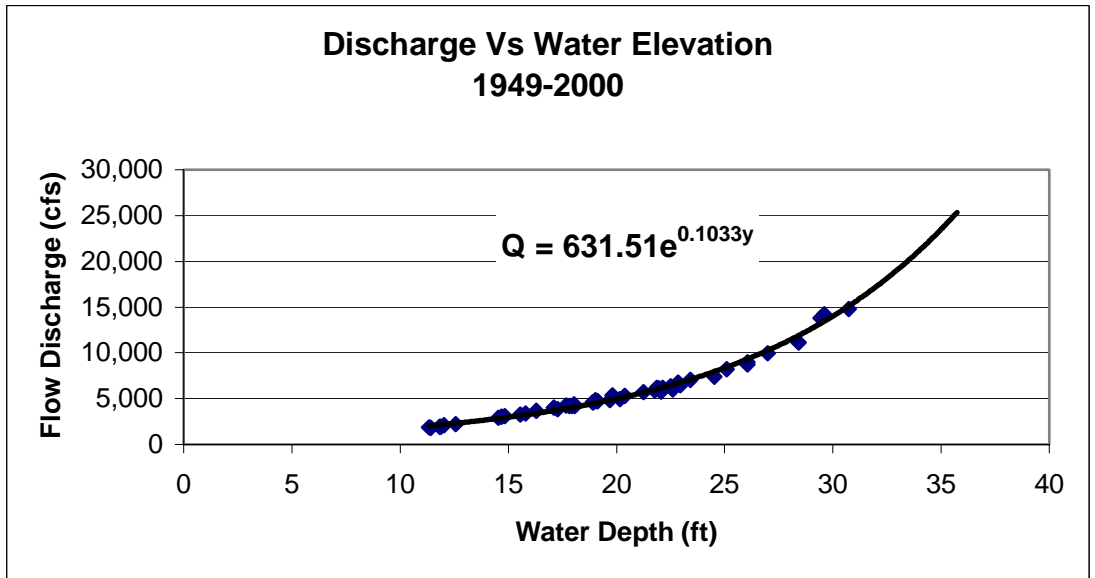


Figure 16. Flow discharge versus water elevation from 1949-2000 (all reported data).

Sediments:

Ardaman & Associates, Inc., the Geotechnical Firm for the Phase II scour analysis project, provided the core samples (from borings S1-2, S2-4, S3-3, and S4-5) for these analyses. Digital photographs of the cores from these borings are given in Appendix B. Logs for the boreholes are presented in Figures 8 and 9. The locations of the boreholes are also shown on the log sheets. As can be seen on the boring logs, once the coring tool reached rock the blow counts became large. Selected core samples were taken from those shown in the photographs in Appendix D for testing in the Rotating Erosion Test Apparatus (RETA) at the University of Florida.

Site Visit:

On July 27, 2001 a site visit was made by Michael Shepard, Hydraulics Engineer with FDOT Dist. 3 in Chipley, FL; Luis Maldonado, Hydraulics Engineer with E.C. Driver and Associates in Tallahassee, FL and D. Max Sheppard with OEA, Inc. and the University of Florida. Photographs taken at the site are located in Appendix C. The water level on this date was low, allowing an inspection of the bed without dive equipment. Continuous rock appeared to be prevalent throughout the riverbed at the bridge site. Bank erosion at and in the vicinity of the bridge site was observed and noted. The sediment in the riverbanks consisted of fine sands typical of this part of Florida. Vegetation on the banks helped resist erosion but in some locations had been overpowered by floodwater flows during low frequency runoff events. It appeared that Piers 3 and 6 on both bridges would be susceptible to erosion and local scour (at least to the depth of the rock layer). These piers are not considered in this analysis since the decision has been made to install scour protection at these locations.

Site Evaluation:

Based on the information obtained at the site, an evaluation of the boring logs, and an examination of the cores from the four boreholes it was decided that a Rate of Erosion analysis of the scour is appropriate for this site. The limestone layer at the channel bed appears to be continuous, approximately horizontal, and of sufficient thickness.

Rate of Erosion Test Results:

Rate of erosion tests were conducted on selected core samples in the Civil and Coastal Engineering Laboratory at the University of Florida in Gainesville, FL. Near bed level cores from bore holes S2-4 and S4-5 were tested along with cores from approximately the same elevation from boreholes S1-2 and S3-3. The results from these tests are summarized in the plots in Figures 17-20 below. Detailed information about the tests is presented in Appendix D. More general information about the initial Rotating Erosion Test Apparatus (RETA) is given in the technical paper in Appendix A.

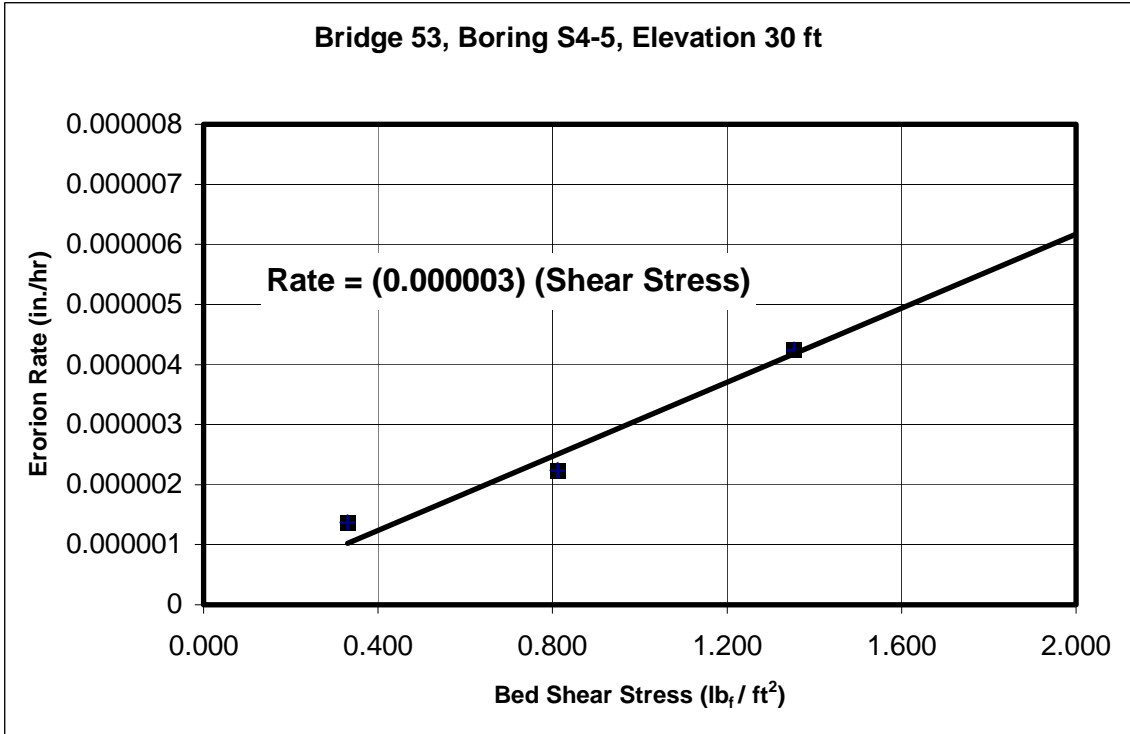


Figure 17. Rate of erosion versus shear stress for core sample No. 1

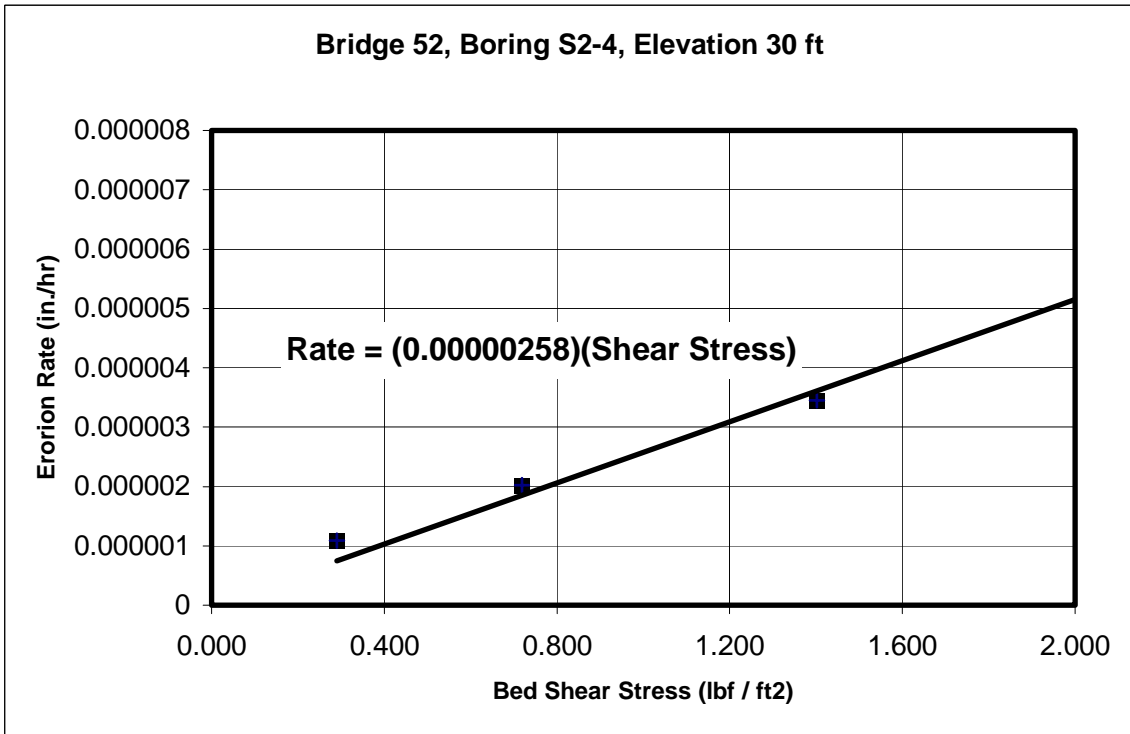


Figure 18. Rate of erosion versus shear stress for core sample No. 2

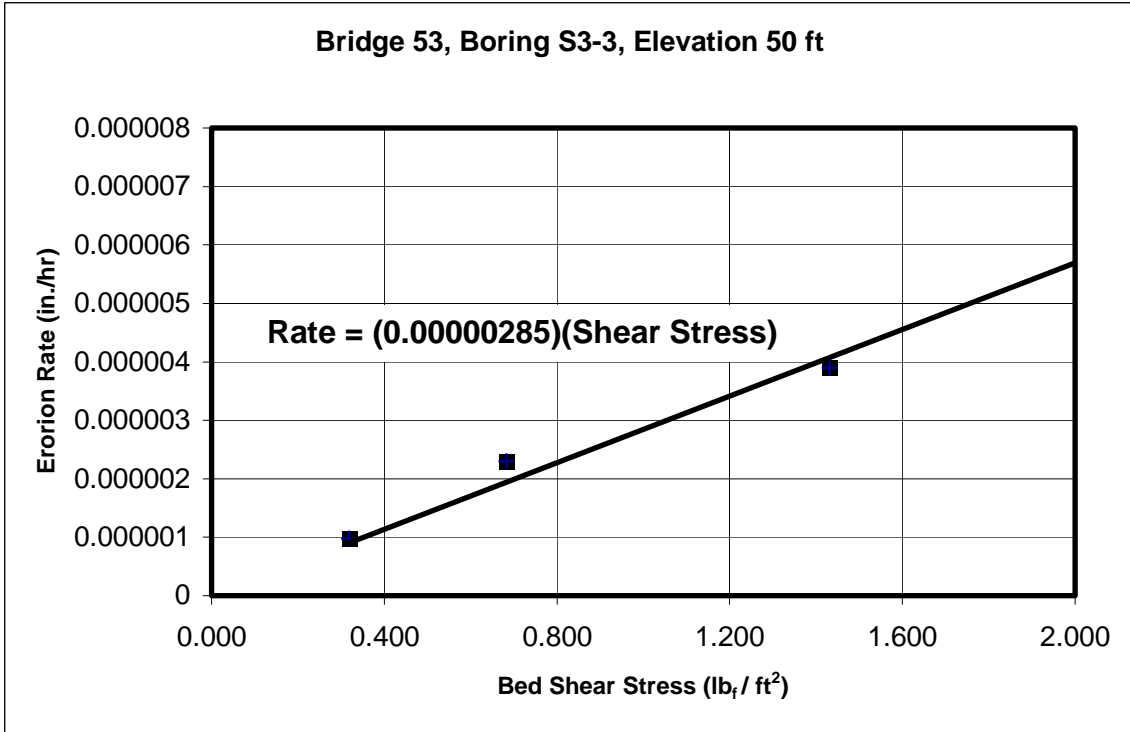


Figure 19. Rate of erosion versus shear stress for core sample No. 3

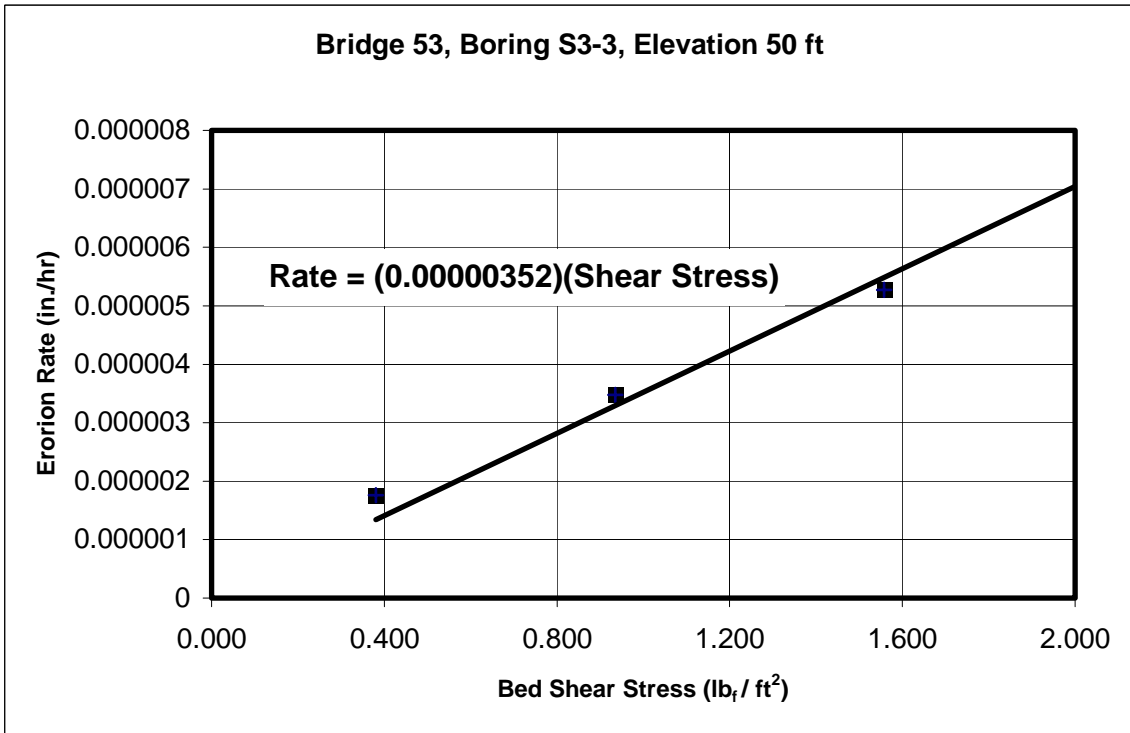


Figure 20. Rate of erosion versus shear stress for core sample No. 4

Analysis:

The procedure for this analysis is given above in the **Approach Taken and Basis for Analysis** section. The first step was to establish conservative hydrographs (i.e. hydrographs with flow velocities and water depths that are greater than anticipated values). Since measured discharge and water elevation data exists for the Chipola River (at a USGS gauge downstream from the I-10 Bridge) this data was compiled and analyzed to determine the accuracy of the regression equation estimates made by David Volkner and Associates, Inc. There is a significant change in the measured discharge versus water elevation at the gauge site around 1948. This is evident from the discharge versus water elevation plots shown in Figures 15 and 16. There is greater than an order of magnitude shift in the coefficient in the trend curves for these two time intervals. The reason for this change is not obvious. Measurement techniques have improved during this time interval and thus there is greater confidence in the latter period (years 1949-2000). During this period there are 51 years of reported data with a maximum reported discharge of 14,800 cfs. The 50 year return interval discharge at the I-10 Bridge site (some 12 miles upstream of the USGS gauge) is 16,605 cfs according to the regression analyses performed by David Volkert and Associates, Inc. This indicates that the regression equation discharge estimates for the I-10 Bridge site are conservative and appropriate for use in generating a projected hydrograph.

To determine the number of the various computed return interval discharge events that occurred during the 51 year record, the daily measured values were scaled up to the predicted values for the I-10 Bridge (i.e. measured values were multiplied by (16,605/14,800)). There are 18,900 daily records from January 1, 1949 to September 30, 2000. This data was analyzed to determine the number of daily discharge occurrences within specified discharge bands. The results are presented in Table 5.

Table 5. Number of occurrences of daily discharges within specified discharge bands for the time interval from January 1, 1949 to September 30, 2000. Data from USGS Gauge No. 02359000 adjusted up to match predicted values at the I-10 Bridge site.

Return Interval Range (yrs)	Discharge Range (cfs)	Number of Occurrences
<1	< 1000	7048
1-2	1,000-4,962	11533
2-10	4,963-10,197	292
10-25	10,198-13,629	18
25-50	13,630-16,606	9
50-100	16,707-19,742	0
100-500	19,743-28,408	0
Total		18900

Since in excess of 50 years of discharge data is available, the projected discharge hydrographs used this data directly and added one 50-year (five day duration) runoff each

year. Every fifth year the 50 year event was replaced by a 100 year event. The I-10 Bridges were constructed in 1976 and their expected life is between 50 and 75 years. Scour calculations are made for 50 years from this date in 5-year increments. Both the upstream depth averaged velocity and the water depth are needed to estimate the bed shear stress in the channel and the maximum shear stress at the piers. The channel average velocity and water depth (as a function of adjusted flow discharge) were estimated from the depth, velocity, and discharge information for the 100 and 500 year flow computations in the Phase II Scour Reports for these bridges. The velocity upstream of the piers was assumed to be twice the velocity estimated from the scour reports. The bed shear stress is computed assuming a hydraulically rough bed and a fully developed logarithmic velocity profile.

$$\tau = \rho \left\{ \frac{V}{2.5 \ln \left[\frac{11.0 y}{k_s} \right]} \right\}^2$$

where

τ \equiv bed shear stress,

ρ \equiv mass density of the water = 62.4 lb_m/ft³,

V \equiv depth averaged velocity,

y \equiv water depth, and

k_s \equiv roughness length = 20 D₅₀ \approx (20) (0.2 mm) / [(25.4 mm/in) (12 in/ft)] = 0.013 ft.

Sample calculation for $y = 12$ ft, $V = 7$ ft/s:

$$\tau = \rho \left\{ \frac{V}{2.5 \ln \left[\frac{11.0 y}{k_s} \right]} \right\}^2 = \frac{(62.4 \text{ lb}_m/\text{ft}^3)}{(32.174 \text{ ft lb}_m/\text{lb}_f \text{ s}^2)} \left\{ \frac{(7.0 \text{ ft/s})}{2.5 \ln \left[\frac{(11.0) (12 \text{ ft})}{0.013 \text{ ft}} \right]} \right\}^2 = 0.18 \text{ lb}_f/\text{ft}^2$$

The 50-year duration daily discharge data set is too large to include in the report but is on the attached CD (file name “Flow Discharge Data”). The computations of the contraction and local scour depths were made with Microsoft EXCEL. This file is also on the CD (file name “Scour Calculations”).

The contraction, local and total scour depths are summarized in Table 6 below.

Table 6. Summary of predicted contraction, local and total scour depths in the near surface layer rock sediments at the I10-Chipola River Bridges.

Year	Contraction Scour Depth (ft)	Local Scour Depth (ft)	Total Scour Depth (ft)
Dec-2006	0.0003	0.0021	0.0024
Dec-2011	0.0008	0.0047	0.0055
Dec-2016	0.0014	0.0083	0.0097
Dec-2021	0.0019	0.0114	0.0133
Dec-2026	0.0024	0.0146	0.0170
Dec-2031	0.0031	0.0186	0.0217
Dec-2036	0.0037	0.0222	0.0259
Dec-2041	0.0042	0.0251	0.0293
Dec-2046	0.0048	0.0290	0.0338
Dec-2051	0.0054	0.0326	0.0380

Summary:

As seen from Table 6 the total scour depths are extremely small in spite of the severe projected hydrograph used for the calculations. The hydrograph was created by scaling up measured discharges from a USGS gauge that is located approximately 12 miles downstream of the I-10 Bridge site. The drainage basins at the I-10 Bridge site and USGS gauge are 587.2 mi² and 781 mi² respectively. A 50-year, 5-day duration discharge was added to the end of each year. Every fifth year the 50-year discharge was replaced by a 100-year discharge. In addition to the scaled up measured flows for the fifty-year period there were 50, 50-year (5-day duration) discharges and 10, 100-year (5-day duration) discharge events.

References:

Annandale, G.W., (1995), "Erodability." Journal of Hydraulic Research, Vol. 33, No. 4, pp 471-493.

Ardaman and Associates, Inc., (1998), Phase I Geotechnical Report Bridge 530052L (Bents 3 and 4), S.R. 8 Over Chipola River, Jackson County, Florida.

Ardaman and Associates, Inc., (1998), Phase I Geotechnical Report Bridge 530053R (Bents 3, 5 and 6), S.R. 8 Over Chipola River, Jackson County, Florida.

David Volkert and Associates, Inc., (1995), Phase I Scour Evaluation Report Bridge No. 530052 I-10 (SR8) Over Chipola River.

David Volkert and Associates, Inc., (1996), Phase II Scour Evaluation Report Bridge No. 530052 I-10 (SR8) Over Chipola River.

David Volkert and Associates, Inc., (1995), Phase I Scour Evaluation Report Bridge No. 530053 I-10 (SR8) Over Chipola River.

David Volkert and Associates, Inc., (1996), Phase II Scour Evaluation Report Bridge No. 530053 I-10 (SR8) Over Chipola River.

HEC-18, (2001), "Evaluating Scour At Bridges", Fourth Edition May 2001. FHWA Publication No. FHWA NHI 01-001.

Henderson, Matthew R., D. Max Sheppard and David Bloomquist, (2000), "A Laboratory Method To Evaluate The Rate Of Water Erosion Of Natural Rock Material", Proceedings of an International Symposium on Scour of Foundations, Melbourne, Australia, November 19, 2000.

Sleath, J.F.A. (1984), "Sea Bed Mechanics", John Wiley and Sons, ISBN 0-471-89091-X.

USGS website

http://water.usgs.gov/nwis/peak?state_cd=12&format=station_list&sort_key=site_no&group_key=NONE&sitefile_output_format=html_table&column_name=agency_cd&column_name=site_no&column_name=station_nm&column_name=lat_va&column_name=long_va&column_name=state_cd&column_name=county_cd&column_name=alt_va&column_name=huc_cd&begin_date=&end_date=&set_logscale_y=1&date_format=YYYY-MM-DD&rdp_compression=file&hn2_compression=file&list_of_search_criteria=state_cd

APPENDIX A
ROCK SCOUR TECHNICAL PAPER

A LABORATORY METHOD TO EVALUATE THE RATE OF WATER EROSION OF NATURAL ROCK MATERIAL

By

Matthew R. Henderson¹, D. Max Sheppard², David Bloomquist³

ABSTRACT

Early bridge scour research has focused on scour of cohesionless sediments around piers. Only recently have researchers started to consider other types of sediments. As a result of an expanding data base for cohesionless sediments (and better understanding of the mechanisms governing scour) engineers in the United States have treated erodible materials as cohesionless sediments for the purpose of scour depth calculations. The equations and techniques presented in the U.S. Federal Highway Administration Bridge Scour Document [FHWA Hydraulic Engineering Circular Number 18 (HEC-18)] for estimating scour depths is based on laboratory studies that were conducted with beds consisting of cohesionless sediments (sand). These equations are known to be conservative for cohesionless sediments and are believed to be overly conservative for erodible rock and cohesive materials. The current approach used in calculating scour depths around structures located in bed materials other than sand is to assume that the bed materials will erode to the same depth as sand given sufficient time. However, bed materials at many bridge sites in the State of Florida are composed of materials other than sand, such as limestone and coquina. These materials can offer a greater resistance to erosion than cohesionless sediments. Hence, a laboratory-based testing device was designed and constructed to evaluate the rates of water erosion of these materials. This device – a rotating cylinder erosion testing apparatus – previously used for testing the erosion of cohesive soils was modified and improved to accept intact rock samples. The new apparatus allows a hydraulic shear stress to be applied to a sample, which simulates the action of water flowing over a bed. The average shear stress can be accurately measured as well as the loss of material due to erosion. Laboratory testing procedures and methods have been developed for conducting the erosion experiments using this apparatus on rock samples. Preliminary experiments were conducted on samples of rock materials collected from bridge sites in Florida

¹ Former Graduate Student - Coastal and Hydraulics Engineer, OEA, Inc., Gainesville, Florida, USA

² Professor of Civil and Coastal Engineering, University of Florida, Gainesville, Florida, USA

³ Associate Professor of Civil and Coastal Engineering, University of Florida, Gainesville, Florida, USA

INTRODUCTION

The current approach used in calculating the scour depths around structures located in bed materials other than sand is to apply the equations provided in HEC-18 with the assumption that the bed materials will erode to the same depths, given sufficient time, as cohesionless sediments (Annandale et al., 1996, p. 59). The limitation of this approach is that it ignores the ability of materials such as rock to offer more resistance to scour than sand (Annandale et al., 1996, p. 59). The sea or riverbeds at a number of bridge sites in the State of Florida are composed of materials other than cohesionless sediments (i.e., other than sand or loose shells). This includes harder materials such as limestone and coquina. The erosion characteristics of these materials are quite different from those of cohesionless sediments. However, due to the current lack of understanding of their erosion characteristics, these rock materials are treated as cohesionless sediments in the current HEC-18 design scour procedures. Since the erosion of rock materials can vary greatly compared to cohesionless sediments, the present approach may be overly conservative in the prediction of scour depths. The Florida Department of Transportation (FDOT) estimates that over designs using these methods have resulted in millions of dollars being wasted on the construction of excessive bridge foundations. Hence, there is a definite need to improve the ability to predict design local and contraction scour depths in erodible rock materials.

CURRENT METHODS TO EVALUATE ROCK EROSION

The FHWA developed an interim guidance to assess rock scourability using empirical methods and testing procedures (Gordon, 1991). These procedures were provided until the results of ongoing research would permit more accurate evaluation procedures.

The guidance recommends the following seven methods to assess the scourability of rock:

- Subsurface Investigation;
- Geologic Formation/Discontinuities;
- Rock Quality Designation (RQD);
- Unconfined Compressive Strength;
- Slake Durability Index;
- Soundness; and
- Abrasion.

The FHWA rock scourability guidance memorandum recommends that design engineers perform several geotechnical tests to evaluate the susceptibility of rock to scour. This memorandum does not provide estimates of the erosion or scour rates of these materials, but provides guidance as to whether the rock materials should be considered a scourable material. The FDOT and University of Florida have conducted some of the recommended tests on rock core samples from bridge sites in Florida to assess their values in relation to the values presented in the guidance document.

Limestone samples collected from the US 441 Bridge site over the Santa Fe River were tested for Unconfined Compressive Strength, Los Angeles Abrasion Test, and Magnesium Sulfate Soundness Test. Statistical analysis of the unconfined compressive strength (q_u) test results indicate that the minimum q_u expected is 1430 kPa or 207 psi (PSI, 1996, p. 5). The Los Angeles Abrasion Test yielded a loss of 72.3% (PSI, 1996, p. 9). The Magnesium Sulfate Soundness Test indicated a loss of 80.0% (PSI, 1996, p. 10).

Tests on limestone samples from a second site produced the following results. The Unconfined Compressive Strength test indicated strengths ranging from 1372 kPa to 1475 kPa (199 psi to 214 psi). Magnesium Sulfate Soundness tests indicated losses from 58.7% to 91.1%.

The guidance memorandum suggests that samples with q_u values below 1725 kPa (250 psi) are not considered to behave as rock (Gordon, 1991). Also, loss rates of 18% from the Magnesium Sulfate Soundness Test can be used as an indirect measure of scour (Gordon, 1991). Rock with loss rates greater than 40% from the Los Angeles Abrasion Test should be considered susceptible to scour (Gordon, 1991). In summary, based on these geotechnical tests, the rock materials in Florida may be susceptible to scour and must be considered in the design and scour protection for bridge sites.

PROPOSED ROCK EROSION PROCESS

A simple but useful definition of rock has been presented in Jumikis (1983):

Rock is a granular material composed of “grains and glue.” There is nothing else involved. The “glue” may be ferroginous, calcareous, argillaceous, or siliceous material, which cements the grains. (Jumikis, 1983, p. 38).

The process of rock erosion by the action of a moving fluid is complex and may be influenced by several factors. The energy imparted by the moving fluid breaks the grains from the glue and subsequently transports the grains downstream. This fundamental description leads to the idea that there is a certain amount of energy required to initiate the erosion of rock. In cohesionless sediments, this concept is known as a critical bed-shear stress. This is the shear stress required to initiate motion of the sediment grains.

Van Rijn (1993) describes the forces acting on a sediment particle resting on a horizontal bed. The fluid forces consist of skin friction forces and pressure forces. The skin friction force acts on the surface of the particles by viscous shear. The pressure force, consisting of a drag and lift force, is generated by pressure differences along the surface of the particle. Particle movement will occur when the moments of the instantaneous fluid forces with respect to the point of contact are just larger than the stabilizing moment of the submerged particle weight (van Rijn, 1993, p. 4.1). In rock materials, there are additional forces that act between the particles tending to maintain the rock as a solid body.

The erosion process in rock can be more complex than just the shear stress acting on a particle. Experimental work performed at the National Research Council of Canada Institute for Marine

Dynamics found that weak sedimentary rock tended to erode by breaking into pieces along fractures, bedding planes, and other internal weaknesses. Cornett et al. (1994) presents a simple model for the hydraulic fracturing of rock. The erosion of the rock at the fracture planes was not directly related to the shear stress. The results of the study suggest that the erosion may be driven by hydrodynamic pressures within fractures (Cornett et al., 1994, p. 26).

Annandale (1995) has developed a method for estimating rock erosion. He suggests the following procedure with regards to hydraulic erosion. This approach is based on a rational correlation between the rate of energy dissipation of flowing water and an erodibility classification of the materials (Annandale, 1995, p. 471). The removal of rock material is perceived as occurring in three stages: jacking, dislodgment, and displacement. Flowing water is subject to turbulence, which, in turn, is associated with a loss in energy. Annandale suggests that turbulence causes pressure fluctuations that result in an action that progressively raises or jacks portions of material from its position. Once removed, the material is then dislodged and displaced (Annandale, 1995, p. 472).

ALTERNATIVE ROCK EROSION PREDICTIVE METHODS

One method developed for use in estimating the erosion of a wide range of materials including rock, and cohesionless and cohesive soils is known as the Erodibility Index method. This method, developed by Annandale (1995), compares a material's ability to resist erosion, which has been designated as the Erodibility Index, with the erosive power of flowing water. The erosive power of water has been defined in terms of the stream power, which is based on the rate of energy dissipation. The primary geotechnical parameters that are used in the calculation of the Erodibility Index are earth mass strength, block or particle size, discontinuity/inter-particle bond shear strength, and the shape of material units and their orientation relative to the flow (Annandale, 1995, p. 481). The comparison of the stream power with the Erodibility Index determines if a material will or will not erode. This method has been further developed for use in estimating the scour at piles for bridges. A description of this method is given in the Interim Report by the Colorado Department of Transportation titled "Preliminary Procedure to Predict Bridge Scour in Bedrock" (Smith, 1994).

SELECTION OF ROCK EROSION TESTING DEVICE

Even though methods have been proposed for predicting water scour of rock materials, much work is still needed. To evaluate the scour of specific types of rock, it is important to examine several factors. First, it is important to understand a material's reaction to fluid flow. A laboratory study is most suited for this type of investigation since it allows better control of important variables and, in general, more accurate measurements. The work performed for this study consisted of the development of a methodology for the evaluation of a rock's erosion rate as a function of the flow of water over its surface. A laboratory-testing device was required to produce the water flow and to measure both the shear stress applied to the surface of the rock sample and the rate of erosion of the sample surface.

Any laboratory method for testing the erosion rates of rock materials, must take the following into consideration:

- There are difficulties in working with rock as a matrix. First, drilling rigs are required to extract samples of rock (termed cores). This is the most common method of collecting rock samples for analysis. Secondly, rock has the propensity to fracture along weak planes, leaving broken pieces. Therefore, the testing device must be able to work with a limited amount of sample material and be able to utilize rock cores that are routinely collected as part of bridge pier design and construction.
- The laboratory-testing device must be able to create flowing water over the rock sample. Specifically, the device must be able to apply a hydraulic shear stress to the rock sample surface.
- Along the same lines as described above, the laboratory-testing device must be able to measure the shear stress that is applied to the sample being tested.
- The testing device must be able to generate shear stresses at levels expected in design storm flow conditions. Therefore, the laboratory-testing device must be able to operate at shear stresses that range from ambient to beyond design conditions.
- Based on information obtained from the literature review, rock can be highly resistant to erosion. Since the erosion rates are very small as compared with cohesionless and cohesive sediments, the laboratory-testing device must be able to accurately measure small amounts of lost material while continuously operating for days.

Based on the above-described criteria, the rotating cylinder erosion testing apparatus was selected. This type of device has been used by several researchers to determine critical stresses and rates of erosion of cohesive sediments. A description of this device, which is similar to the Couette viscometer, is given below.

PREVIOUS USE OF ROTATING CYLINDER APPARATUS

Moore and Masch (1962) applied the rotating cylinder principle used in viscometers to measure the scour resistance of cohesive soils. The device was called the rotating cylinder erosion test apparatus. A cylindrical sample of cohesive sediment was suspended inside a larger circular cylinder. The outer cylinder is free to rotate about its axis. The annular gap between the cylinder and sample was filled with fluid. As the outer cylinder is rotated, momentum is imparted to the fluid and the fluid moves, imparting a shear stress to the face of the sample. The cohesive soil sample is stationary but mounted on flexure pivots so that the shear stress transmitted to the sample surface resulted in a slight rotation of the supporting tube. The resulting rotation was calibrated to measure the torque on the sample from which the shear stress could be computed (Moore and Masch, 1962, p. 1444).

As a shear stress was applied to the sample, material was eroded from the face of the sample. The amount of material eroded was measured and the duration that the shear stress was applied was also recorded. From this information, the average rate of erosion could be computed for a given applied shear stress.

Several researchers including Rektorik et al. (1964), Arulanandan et al. (1973), Sargunam et al. (1973), Alizadeh (1974) and Chapius and Gatien (1986) have used similar devices with improvements and enhancements. Akky and Shen (1973) used the rotating cylinder apparatus developed by Arulanandan to evaluate the erosion of cement-stabilized soil. In fact, Chapius and Gatien improved the testing apparatus to accept either intact or remolded cohesive soils, with improved rotation guidance, better alignment, a lower internal friction, and a reduction of the influence of end conditions on the fluid annular flow (Chapius and Gatien, 1986, p. 86). These researchers evaluated the rate of erosion of cohesive sediments with the rotating cylinder device.

THEORETICAL ASPECTS OF THE ROTATING CYLINDER APPARATUS

Essentially, the rotating cylinder works along the same principle as a rotational viscometer. Rotational viscometers operate on the principle that when a cylinder is suspended and immersed in a liquid contained in a vessel which rotates at a constant speed, a balancing couple will be required to keep the cylinder at rest. This couple may be produced by the torsion of a wire from which it is suspended (Merrington, 1949, p. 30).

For a Newtonian fluid, the velocity increases almost linearly from zero at the stationary inner cylinder (no-slip condition) to the velocity of the outer rotating cylinder at the wall of the outer cylinder. For low rotational speeds this approximates laminar flow between two infinite parallel plates. The near linear velocity profile between the two concentric cylinders only occurs during low velocity, laminar flow conditions. As the speed of the outer cylinder is increased, there are changes in the flow regime. The flow begins as a laminar flow but becomes unstable as the velocity increases. The instability grows until a secondary flow is achieved. The secondary flows, described by G.I. Taylor, are a succession of stable toroids or vortices, which have been termed Taylor's rotational vortices. These vortices are well-defined counter-rotating circulation cells. As the outer cylinder speed is increased even further, the Taylor vortices become unstable and ultimately the flow is uniformly turbulent.

Rohan and Lefebvre (1991) investigated certain hydrodynamic aspects of the rotating cylinder erosion tests. The critical Reynolds number between laminar flow and the formation of the above-mentioned Taylor vortices can be calculated. (Rohan and Lefebvre, 1991, p. 167). In fact, there are three regimes of flow that can be distinguished based upon the calculation of the Taylor number (Rohan and Lefebvre, 1991, p. 169):

1. $Ta < 41.3$ = laminar Couette flow;
2. $41.3 < Ta < 400$ = laminar flow with Taylor vortices, and
3. $Ta > 400$ = turbulent flow.

In cases where the flow consists of secondary flows (vortices) or turbulent flow, the velocity profile is no longer a linear relationship from the wall of the stationary inner cylinder to the rotating outer cylinder.

ADVANTAGES AND LIMITATIONS OF TESTING DEVICE

The rotating cylinder test apparatus met several of the design criteria presented above. Specifically:

- a small sample of rock can be used in this type of device as the outer cylinder can be sized to accommodate the size of standard rock cores,
- a flowing water generated shear stress can be applied to the sample,
- the average shear stress on the sample can be measured by measuring the torque that is being applied to the sample,
- small quantities of material being eroded can be measured using precision balances, and
- the apparatus can be operated for long periods of time as the outer cylinder can be driven by a continuous duty motor.

It is also important, however, to discuss the limitations of this type of testing device to understand where uncertainty and bias may be present in the results. The shear stress is computed by measuring the torque on the sample. However, the torque being measured is the torque being applied to the entire sample. Therefore, the calculation of the shear stress results in the average shear stress over the entire sample surface. The results from the experiments assume that the shear stress is uniform across the entire surface of the sample. In actuality, the surface of rock samples can be pitted and uneven. Therefore, there may be variations in the shear stress distribution over the face and thus local shear stresses are likely to be greater than the averaged value computed from the moment on the sample.

In summary the shear stress computed from the measured torque may be biased in the direction of underestimating the shear stress acting on the sample. In addition to the variations in the shear stress over the sample surface there may also be components of the flow acting in directions other than the direction in which the torque is being measured. Thus, there may be a component of shear stress that is eroding the surface of the sample that is not being accounted for in the measurements. In the application of these results, the underestimation of shear stress would provide conservative estimates of the rates of erosion versus shear stress. That is, the results would show greater erosion rates for a given shear stress. The conservative nature of these results would be appropriate for design applications.

ROTATING CYLINDER APPARATUS

The rotating cylinder testing apparatus used in this study was similar to the devices previously used; however, some modifications have been made. Figures 1 and 2 are schematic drawings of the rotating device and Figure 3 is a photograph of the actual device. English units are shown for equipment dimensions as they were used by manufacturers to specify equipment sizes. The metric equivalents were also provided. The major components of the apparatus consist of the following:

- Bodine 1/8-hp Frame 42A motor (2500 RPM at 50 in-oz [353 mm-N] of torque) with controller,
- 3-in (7.62-cm) outside diameter (2.5-in [6.35-cm] inside diameter) acrylic cylinder,
- Omega digital readout, and
- Sensotec Model QWFK-8M Miniature Reaction Torque Transducer (torque cell) with a range from 0 to 25 in-oz (0 to 176.5 mm-N).

The testing apparatus consists of a prefabricated metal stand with a motor access panel placed on the front of the stand. The prefabricated metal stand has adjustable feet, which is used to level the apparatus, and handles mounted to the sides that can be used to transport the device. The motor is mounted beneath the top of the prefabricated metal stand. The acrylic cylinder is mounted to a 1/2-in (1.27-cm) diameter steel shaft that extends beneath the top of the metal stand. Two pulleys and a belt connect the motor and shaft. The motor controller is mounted on the outside of the access panel.

The rock sample to be tested is fixed between 2 thin plates and is secured by a 3/16-in (0.48-cm) threaded rod placed through the center of the sample. The rock sample/rod system is connected to the torque cell, which is held stationary by the support bracing fixed directly to the apparatus. The output from the torque cell is displayed by the Omega digital readout, which was programmed (following the manufacturers' recommended procedures) to provide the torque output in N-mm. The readout is mounted on the outside of the access panel next to the motor controller. A tare switch is connected to the readout. This allows the readout to be set to zero before a test to facilitate the torque reading. The tare switch is also mounted on the face of the access panel just below the readout.

The addition of the torque cell is an improvement over the previous methods for measuring torque. The torque cell allows for the elimination of bearings or flexure pivots to support the sample and for the measurement of the torque contributions due to end effects. In the previous devices, the cohesive soil sample was mounted on pivots or bearings so that the shear stress transmitted to the sample surface resulted in a slight rotation of the supporting tube. The resulting rotation was calibrated to measure the torque on the sample by using either torsion wires or by a pulley and weight system. In this type of set-up, the friction within the bearings must be accounted for.

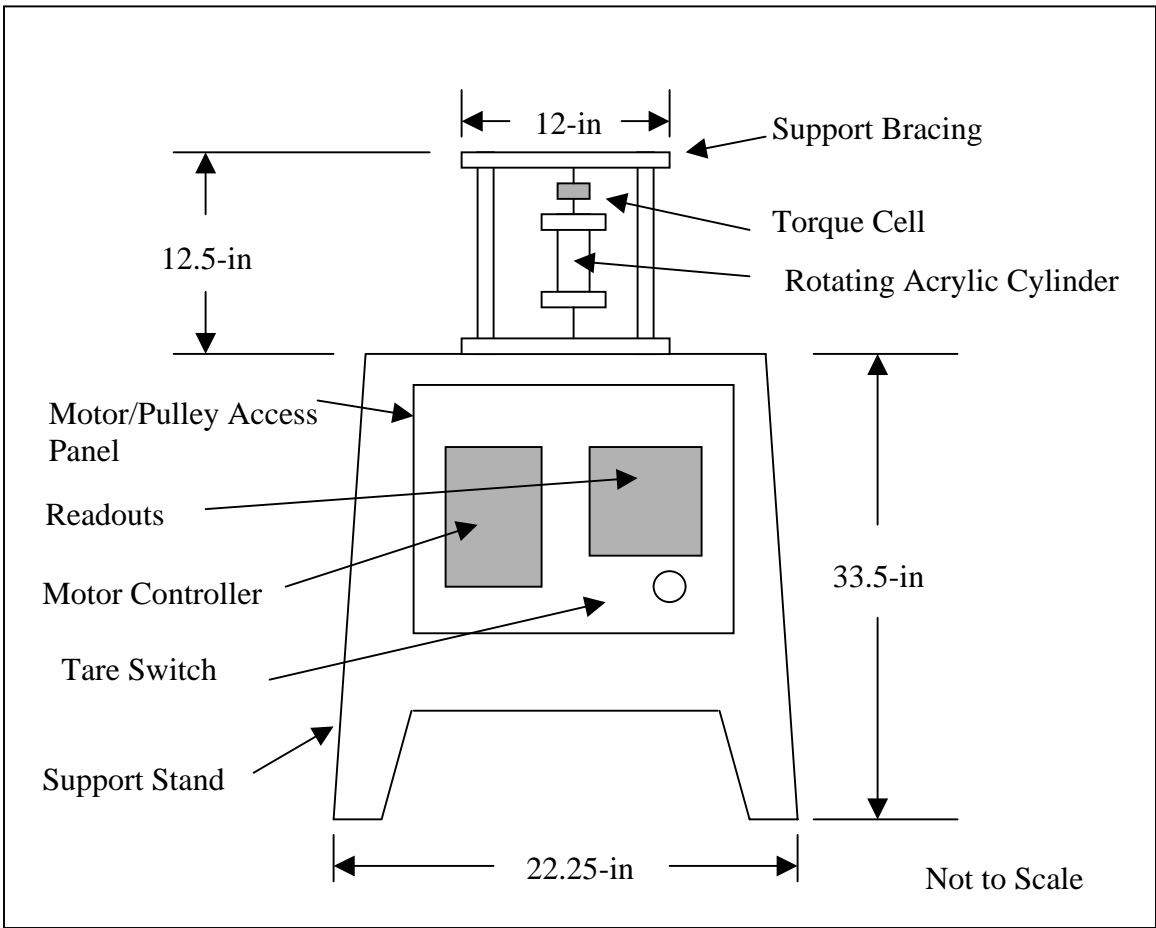


Figure 1. Rotating Cylinder Test Apparatus Schematic

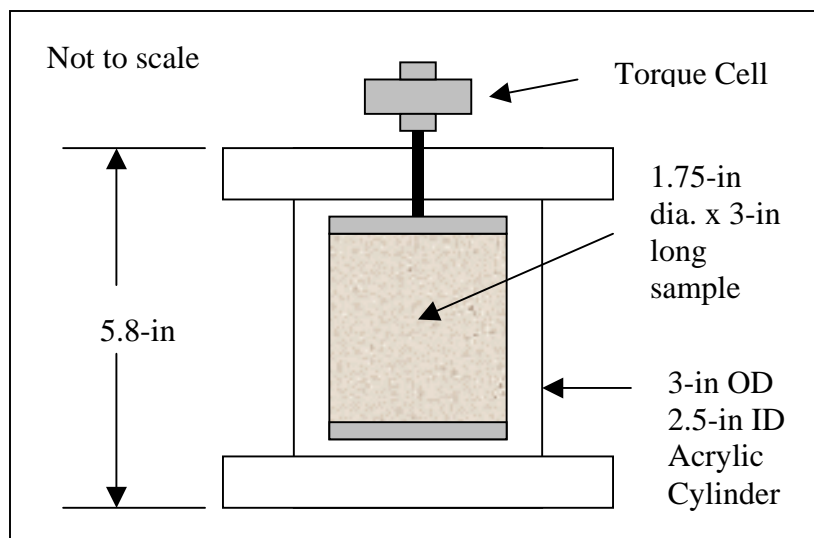


Figure 2. Schematic of Acrylic Cylinder and Torque Cell



Figure 3. Rotating Cylinder Test Apparatus

The addition of the torque cell allows for the direct measurement of torque with minimal rotation of the sample. Thus the need for bearings is eliminated. One end of the torque cell is mounted to the fixed support bracing and the sample is mounted to the other end.

To calibrate the torque cell, a moment arm was attached to the shaft where the sample would normally be located. A wire was run from the moment arm, over a pulley, to a pan where brass weights were placed. This allowed a known torque to be placed on the torque cell. The torque reading was plotted versus the expected value.

DETERMINATION OF END EFFECTS

In this type of erosion testing device, the torque measurements of interest are for the net torque exerted on the sample. Water flow over the top and bottom ends of the sample also produces a torque that is measured by the torque cell. Since the ends are protected from being eroded by thin metal plates, the torque being produced on the end of the sample must be taken into consideration. A method to evaluate the end effects with the torque cell was developed.

Experiments were performed to measure the torque exerted on the bottom plate. The experiments consisted of placing the threaded rod with the bottom plate only within the acrylic

cylinder. Enough water is added in the rotating cylinder at each RPM tested to cover the underside of the bottom plate only. The torque at each RPM tested was recorded and a plot was developed. As will be discussed in the experimental procedures section, the torque on the bottom plate for a given RPM can be obtained from the plot. This torque is subtracted from the total torque reading. It should be noted that during a particular erosion test, only enough water is added to the cylinder annulus to wet the sides and not the end plate on the top of the sample. Therefore, only the end effects from the bottom plate needed to be considered.

EXPERIMENTAL SAMPLE PREPARATION

Samples that were tested in the apparatus were collected from rock cores obtained by the FDOT. The sample was formed by drilling a horizontal solid cylinder through a vertical core. The rationale for collecting a sample from the side of a core was based on the results of a preliminary experiment performed at the University of Florida. A sample of limestone was collected from a FDOT core and then cut into a cube. To obtain qualitative information about the anisotropy of these samples, a pressure washer was directed at each face of the sample. While this does not simulate field conditions (tangential flow over a bed), it did provide some insight into the erosion properties of the sample. It was discovered that there were differences in the rates at which various faces eroded. These differences in erosion can be attributed to the non-homogeneity and anisotropy of rock samples. It was concluded that in order to most accurately simulate the field condition, the sample face being eroded should be in the same orientation as in the field. By cutting a horizontal solid cylinder from the core, the eroding surface will be closer to the field situation.

The samples for erosion testing were taken from 4-in (10.16-cm) nominal diameter cores collected by the FDOT. The samples were cored from the sides using a concrete wet corer with a 2-in (5.08-cm) diameter core bit. This produced a sample of 1.75-in (4.45-cm) in diameter. The ends of the sample were leveled with a concrete wet saw. This left a sample with a length of approximately 3-in (7.62-cm).

A hole must be drilled in the center of the rock material to connect the end plates as well as to allow the sample to be connected to the torque cell. In preparing the samples, it was discovered that during coring, the samples could easily fracture. To minimize the fracturing, a 3/16-in (0.48-cm) diameter hole was drilled through the center. This minimized the disturbance to the sample and kept the sample intact.

EXPERIMENTAL PROCEDURE

The following is the procedure used to conduct a typical erosion test.

Sample Preparation

1. Prepare the sample for erosion testing as described in above by using a concrete wet corer and masonry drill bit.
2. Record the mass of the sample with the mass balance.

3. Place the sample in the drying oven for at least 16 hours to dry. After that time, record the mass of the sample. The sample is considered dry when the mass change is less than 0.1% in a period greater than 1 hour. Record the sample dry mass.
4. Measure the diameter of the sample with a Pi Tape at a minimum of three locations with the calipers and record the average diameter of the sample.
5. Measure the length of the sample with the calipers.
6. Measure the volume of the sample by gently submerging the sample in a graduated cylinder and measure the volume of water displaced.
7. Compute the sample dry density from the above measurements in g/cm^3 .
8. Collect the water and loose material in a drying dish. Place the drying dish in the drying oven to remove the water. Record the mass of remaining material.
9. Completely immerse the sample in water for at least 16 hours to hydrate. The sample is hydrated to simulate a saturated rock formation as may be found in a waterway bed. After that time, record the mass of the sample. The sample is considered hydrated when the mass change is less than 0.1% in a period greater than 1 hour.

Testing Procedure

1. Secure sample on the threaded rod with the platens and place the sample in the rotating cylinder erosion-testing device.
2. Fill the rotating cylinder annulus with water to the proper level. It is important to note that water from the actual field site where the sample was collected should be used.
3. Place the rubber stopper on the acrylic cylinder and then attach sample to torque cell.
4. Set the offset of the torque cell with the tare switch to 0.000 mm-N.
5. Turn on the motor and increase the RPM (as measured by the tachometer) until the desired torque is achieved.
6. Allow the test to run for a minimum of 72 hours. Record the duration of the experiment in min with the stopwatch. Periodically adjust the motor speed to keep a constant torque on the sample. Record the torque in mm-N applied to the sample.
7. Turn off the motor and allow the water within the annulus to cease motion.
8. Remove the sample from the torque cell and cylinder.
9. Empty the water out of the cylinder and clean out the eroded particles in the cylinder.
10. Place the sample in the drying oven for at least 16 hours to dry. After that time, record the mass of the sample. The sample is considered dry when the mass change is less than 0.1% in a period greater than 1 hour. Record the sample dry mass.

There are a few important items to note with regards to the experimental procedures. First, prior to beginning the actual erosion experiments, a preparation run is required. The preparation run is required to remove loose material from the surface of the rock sample prior to measuring the erosion. The coring process disturbs the surface of the sample and this may cause an excessive amount of material to erode that may not have eroded otherwise. The preparation run was conducted after the sample dimensions were recorded but prior to the first experiment.

Also, at times, a slight amount of material would be removed from the sample during the saturation process. This material was collected and weighed (dry weight). This value was then

subtracted from mass lost prior to the experiment so the change in mass would reflect the amount of material lost during the experimental run.

EXPERIMENTAL RESULTS

The first experiment was conducted on a rock sample from the site of the 17th Street Temporary Bridge crossing of the Intracoastal Waterway in Fort Lauderdale, Florida. The boring log that accompanied the sample described the rock as a “Loose Cemented Sand”. The sample was collected from a proposed bridge pier location at a depth interval of 27.92 m and 30.97 m (91.58 ft and 101.58 ft) below the mudline. The second experiment was conducted on a rock sample from the same bridge site but at a different pier location. The boring log that accompanied this sample described the rock as a “Dark tan sandstone with small voids and no shells.” The sample was collected from a depth interval of 29.93 m and 30.54 m (98.18 ft and 100.18 ft) below the mudline. This sample was collected at the same bridge location as the Cemented Sand sample but at a different pier location. At the time of this paper submission two tests were performed with the Sandstone and four with the Cemented Sand.

Figure 4 is a plot of both the Loose Cemented Sand and Dark Tan Sandstone erosion data. A trend line was fitted through the Cemented Sand data using Microsoft Excel. The Cemented Sand and Sandstone samples were similar in appearance and texture. This linear relationship is based on only four data points for the Cemented Sand. Research conducted by Chapius and Gatien in the area of cohesive soil erosion found that between six and ten samples were required to be tested to achieve a good evaluation of the erodibility of a clayey material. This number of samples allows for a statistical determination of the critical shear stress and the mean erosion rate as a function of shear stress (Chapius and Gatien, 1986, p. 86).

Rock is a non-homogenous and anisotropic material. It is anticipated that, similar to the findings Chapius and Gatien, that several samples from a given site must be tested before a meaningful erosion rate versus bed shear stress relationship can be developed. Therefore, the results presented here are preliminary, as only one sample was tested. The test results have the anticipated trend but a number of additional tests are needed before the variability of the samples and the locus of highest values can be established.

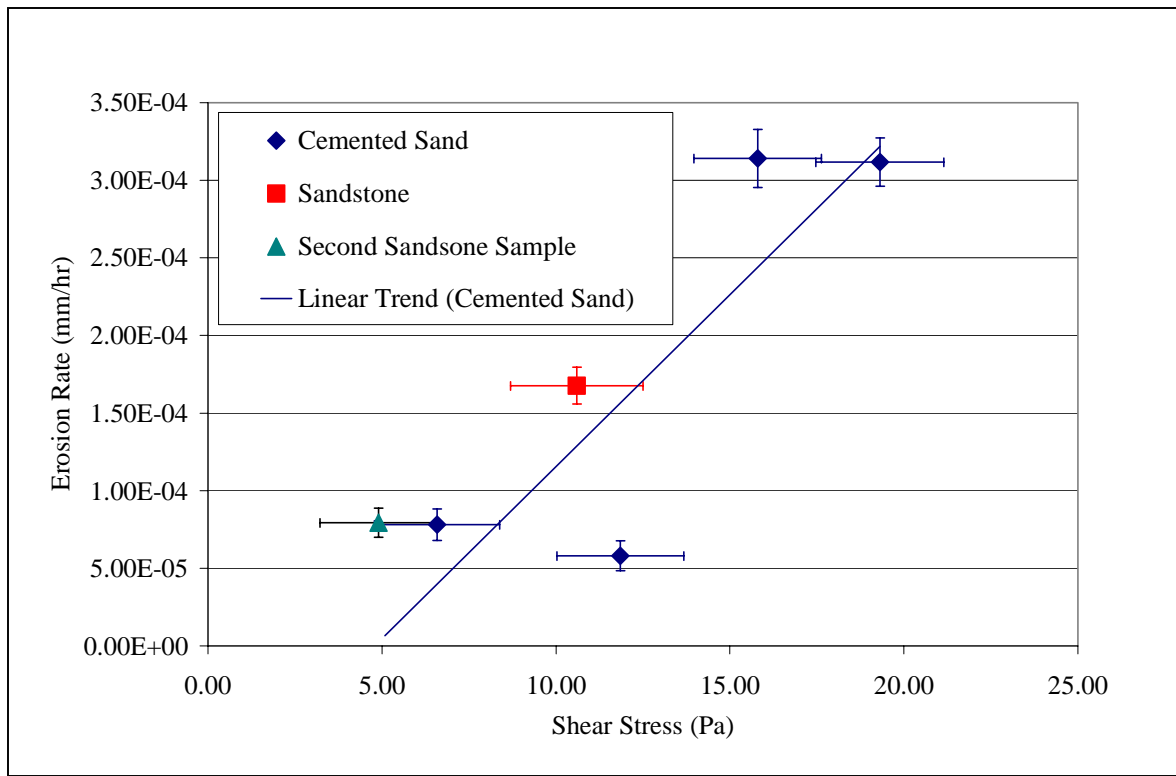


Figure 4. Cemented Sand and Sandstone Erosion Rate Data

CURRENT RESEARCH

Currently, an improved multiple rotating cylinder device is being constructed to allow for several samples to be tested at varying shear stresses simultaneously. The improved device incorporates recommended design changes identified during the prototype construction and testing process. Also, another flume for the purpose of measuring erosion rates in rock materials is being constructed. In this device, water is circulated through a closed rectangular duct over the face of a rock sample. The face of the sample is advanced upward so as to maintain it flush with the bottom of the flume. This is an attempt to better simulate the *in-situ* conditions with water flowing over a natural bed. The results from this device will be used to compare and contrast with the data from the rotating cylinder apparatus.

ACKNOWLEDGEMENTS

This work was funded by the Research Office of the Florida Department of Transportation. Technical coordination was provided by the State Drainage Engineer, Mr. Shawn McLemore. We appreciate his support and technical input to the research. We also wish to thank Dr. Dave Horhota and Mr. Rick Renna of the Florida Department of Transportation for providing rock samples. Thanks go to Dr. Rob Nairn, of Baird & Associates, and Dr. Andrew Cornett, of the Canadian Hydraulics Center, for providing information on their rock erosion experiments. Judy Mitrani and Ken Kerr assisted with the experimental work and sample collection.

REFERENCES

- Akky, M.R., and Shen, C.K., 1973. "Erodibility of a Cement-Stabilized Sandy Soil." Soil Erosion: Causes and Mechanisms; Prevention and Control, Conference Workshop on Soil Erosion, Highway Research Board Special Report 135, Washington, DC, pp. 30-41.
- Alizadeh, A., 1974. "Amount and Type of Clay and Pore Fluid Influences on the Critical Shear Stress and Swelling of Cohesive Soils." Ph.D. dissertation, University of California, Davis.
- Annandale, G.W., 1995. "Erodibility." Journal of Hydraulic Research, Vol. 33, No. 4, pp. 471-493.
- Annandale, G.W., Smith, S.P., Nairn, R., and Jones, J.S., 1996. "Scour Power." Civil Engineering, American Society of Engineers, July, pp. 58-60.
- Arulanandan, K., Sargunam, A., Loganathan, P., and Krone, R.B., 1973. "Application of Chemical and Electrical Parameters to Prediction of Erodibility." Soil Erosion: Causes and Mechanisms; Prevention and Control, Conference Workshop on Soil Erosion, Highway Research Board Special Report 135, Washington, DC.
- Chapius, R., and Gatien, T., 1986. "An Improved Rotating Cylinder Technique for Quantitative Measurements of the Scour Resistance of Clays." Canadian Journal of Geotechnical Engineering, Vol. 23, pp. 83-87.
- Cornett, A., Sigouin, N., and Davies, M., 1994. "Erosive Response of Northumberland Strait Till and Sedimentary Rock to Fluid Flow." National Research Council of Canada, Institute for Marine Dynamics, TR-1994-22, September, Ottawa, Canada, pp. 1-15, 26-27.
- Gordon, S., 1991. "Scourability of Rock Formations." Federal Highway Administration Memorandum, July 19, Washington, DC.
- Jumikis, A.R., 1983. Rock Mechanics. 2nd ed., TRANS TECH Publications, Clausthal-Zellerfeld, Federal Republic of Germany, pp. 37-45, 51-53.
- Merrington, A.C., 1949. Viscometry. Edward Arnold, London, England, p 30.
- Moore, W.L. and Masch, F.D., 1962. "Experiments on the Scour Resistance of Cohesive Sediments." Journal of Geophysical Research, Vol. 67, No. 4, April, pp. 1437-1446.
- PSI – Professional Services Industries Inc., 1996. Preliminary Geotechnical Engineering Study, U.S. 441 Bridge Over Santa Fe River, WPI No. 2110486, October 10, pp. 2-10.

- Rektorik, R.J., and Smerdon, E.T., 1964. "Critical Shear Stress in Cohesive Soils from a Rotating Shear Stress Apparatus." Paper No. 64-216, American Society of Agricultural Engineers, June.
- Richardson, E.V. and Davis, S.R., 1995. "Evaluating Scour at Bridges." 3rd ed., Hydraulic Engineering Circular No. 18, Publication No. FHWA-IP-90-017, Office of Technology Applications, HTA-22, Washington DC.
- Rohan, K. and Lefebvre, G., 1991. "Hydrodynamic Aspects in the Rotating Cylinder Erosivity Test." Geotechnical Testing Journal, Vol. 14, No. 2, June, pp. 166-170.
- Sargunam, A., Riley, P., Arulanandan, K., and Krone, R.B., 1973. "Effect of Physicochemical Factors on the Erosion of Cohesive Soils." Journal of the Hydraulic Divisions, Proceedings of the American Society of Civil Engineers, Vol. 99, No. HY3, March, pp. 555-558.
- Smith, S.P., 1994. "Preliminary Procedure to Predict Bridge Scour in Bedrock." Colorado Department of Transportation, Report No. CDOT-R-SD-94-14, Denver, CO, December.
- Van Rijn, L.C., 1993. Principles of Sediment Transport in Rivers, Estuaries, and Coastal Seas. Aqua Publications, Amsterdam, The Netherlands, p. 4.1.

APPENDIX B
PHOTOGRAPHS OF SEDIMENT CORES



Figure B1. Photograph of core samples from Borehole S1-2.



Figure B2. Photograph of core samples from Borehole S1-2.



Figure B3. Photograph of core samples from Borehole S1-2.



Figure B4. Photograph of core samples from Borehole S1-2.

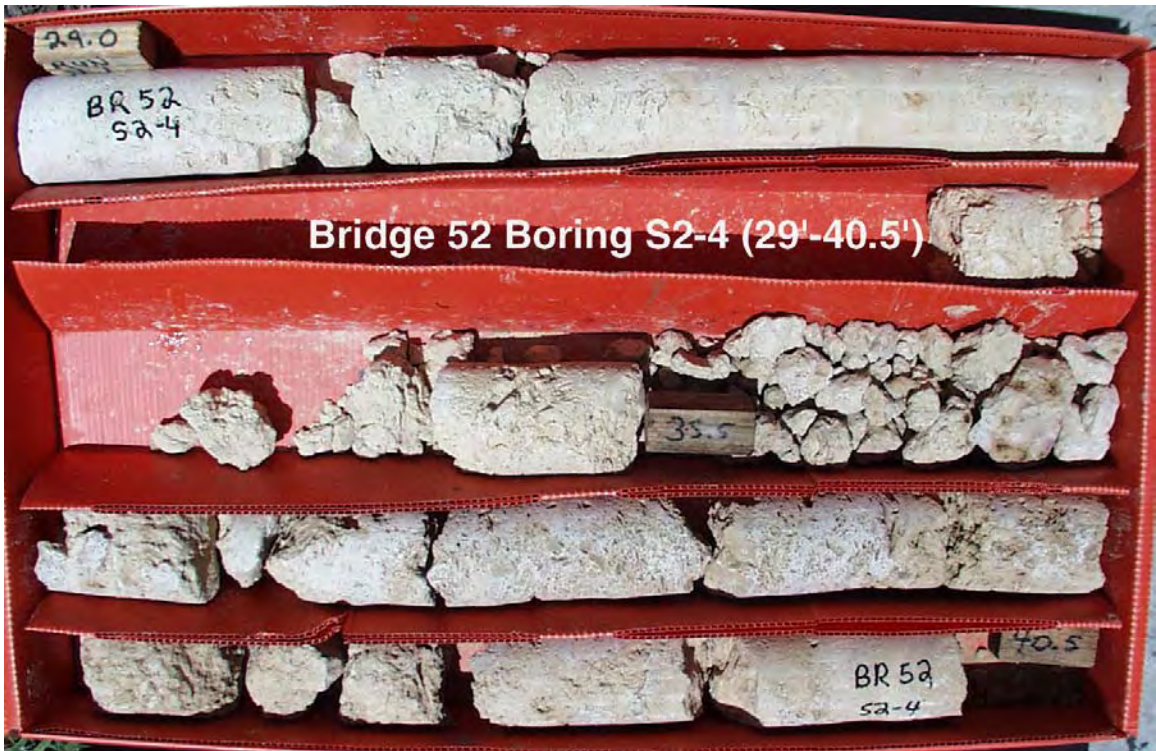


Figure B5. Photograph of core samples from Borehole S2-4.



Figure B6. Photograph of core samples from Borehole S2-4.



Figure B7. Photograph of core samples from Borehole S2-4.



Figure B8. Photograph of core samples from Borehole S2-4.



Figure B9. Photograph of core samples from Borehole S3-3.



Figure B10. Photograph of core samples from Borehole S3-3.



Figure B11. Photograph of core samples from Borehole S3-3.



Figure B12. Photograph of core samples from Borehole S3-3.



Figure B13. Photograph of core samples from Borehole S4-5.



Figure B14. Photograph of core samples from Borehole S4-5.

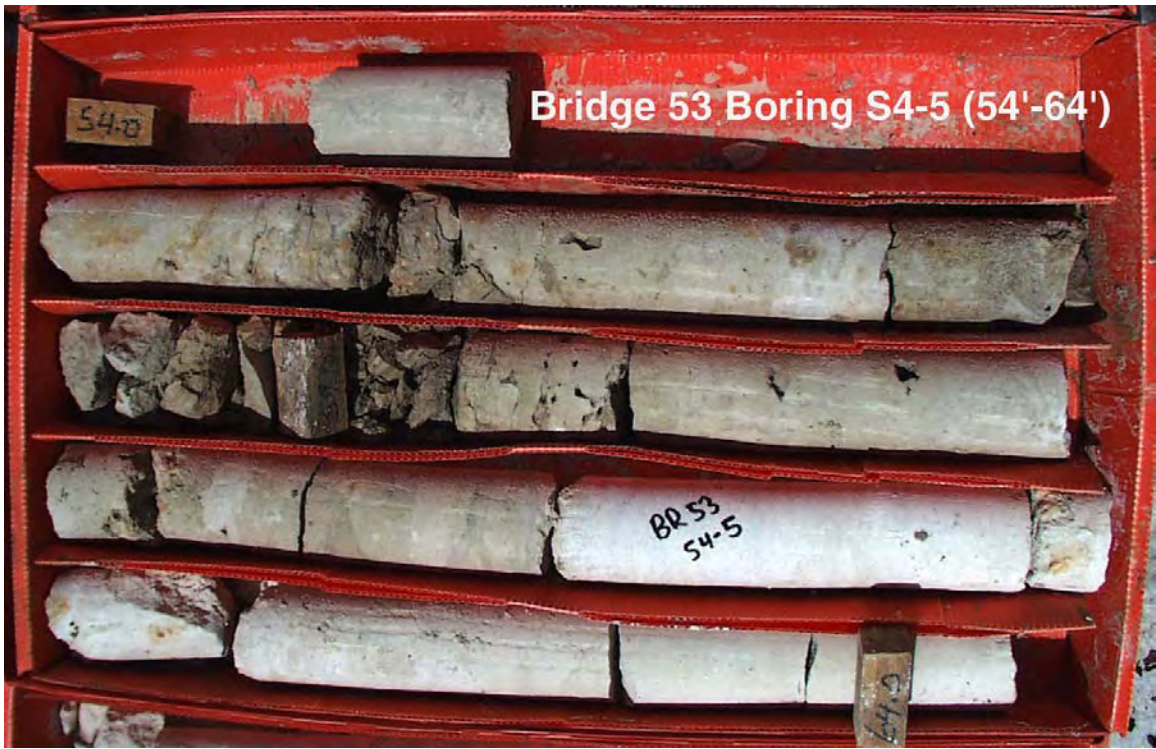


Figure B15. Photograph of core samples from Borehole S4-5.



Figure B16. Photograph of core samples from Borehole S4-5



Bridge 53 Boring S4-5 (82'-87')

NO. 17-560- NS-10 DIVIDER

Figure B17. Photograph of core samples from Borehole S4-5.

APPENDIX C

PHOTOGRAPHS TAKEN DURING SITE VISIT



Figure C 1. Bridge 52 East Abutment



Figure C 2. Bridge 52 Looking West 3.



Figure C 3. Bridge 53 Looking East 2.



Figure C 4. Bridge 53 Looking West 2.

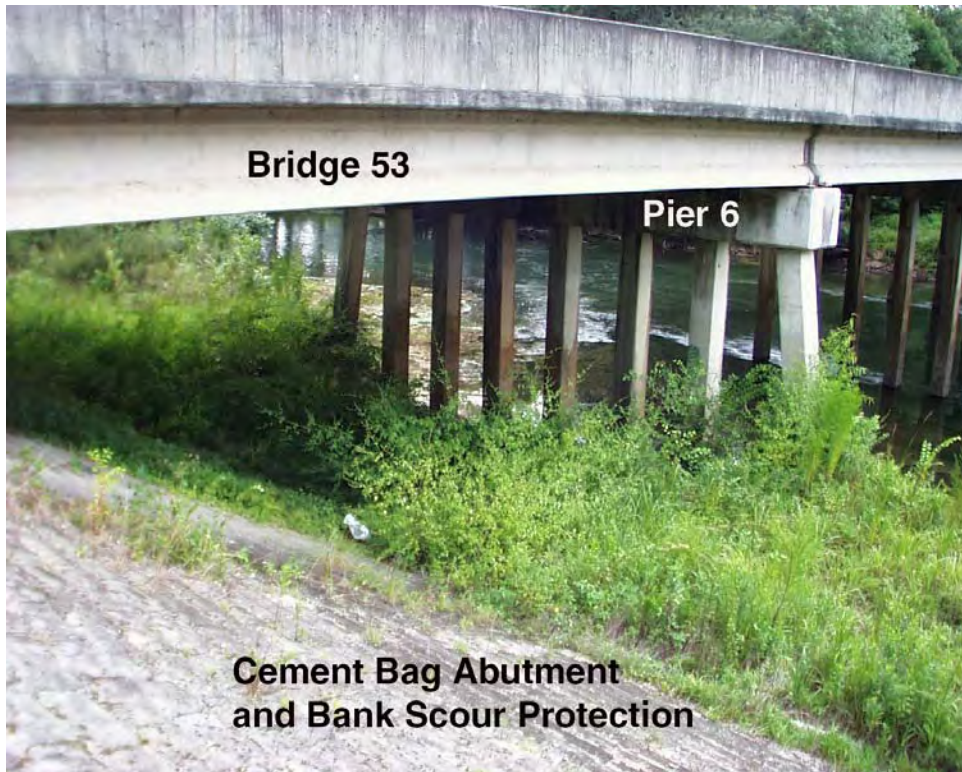


Figure C 5. Bridge 53 Looking West 4

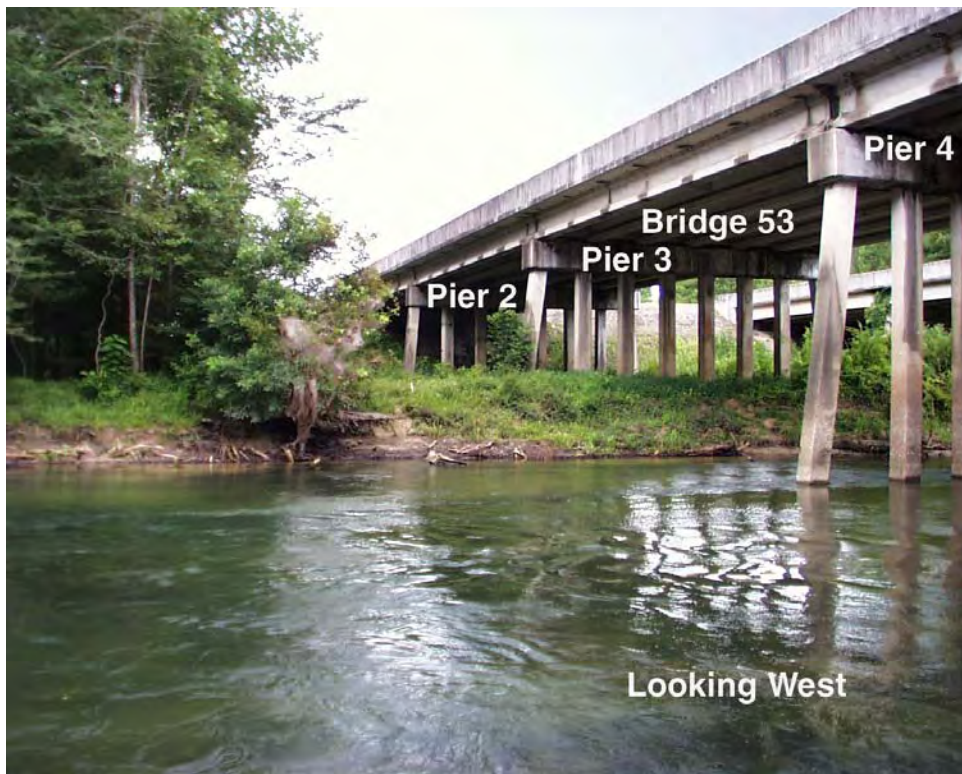


Figure C 6. Bridge 53 Looking West.



Figure C 7. Bridges 52 and 53 East Ends.

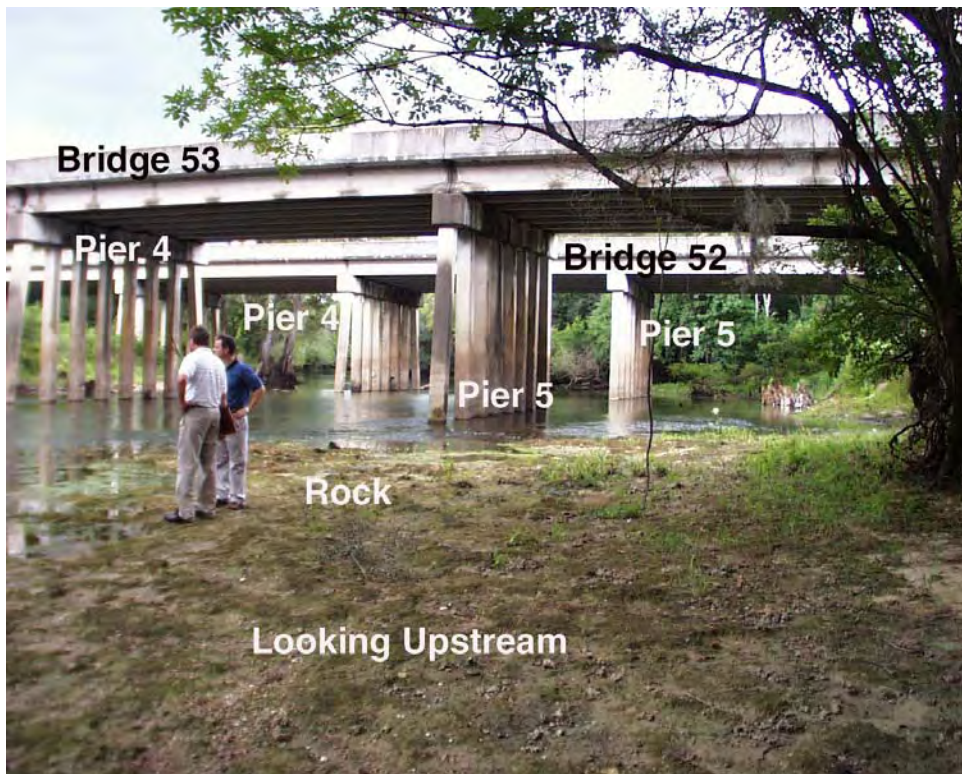


Figure C 8. Bridges 52 and 53 Looking Upstream 2.

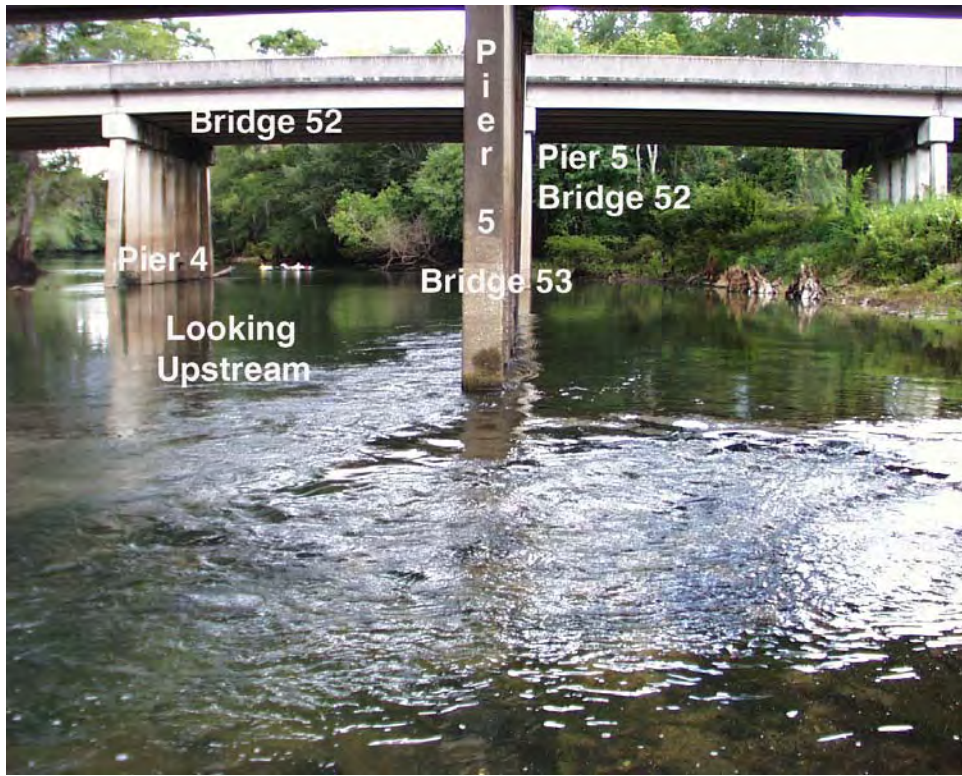


Figure C 9. Bridges 52 and 53 Looking Upstream.



Figure C 10. Bridges 52 and 53 Looking West.

APPENDIX D

**RETA
TEST PROCEDURE, PHOTOGRAPHS
AND
TEST RESULTS**

TEST PROCEDURE

Sample Preparation Procedures for FDOT Design Cores

1. Cut the 6 cm diameter FDOT rock core to a length of about 4" using the core holding apparatus as described before in this section.
2. Drill a 1/4" hole through the center of the sample with a masonry drill bit using the new drilling procedure described below.

Sample Preparation Procedures for FDOT Construction Cores

1. Core a 1.75" sample from the 4" FDOT rock core using a concrete wet corer with a 2" diameter bit.
2. Cut sample to a length of about 3" using the core holding apparatus.
3. Drill a 3/16" hole through the center of the sample with a masonry drill bit using the new drilling procedure described below. (Note: the specimen holding apparatus for this diameter core is being constructed in the next phase of this project)

New Drilling Procedure

1. Place the sample into the retaining device and be sure that the top of the sample rests flush against the bottom side of the drilling template.
2. Tighten the lower strap around the sample so that the sample is securely fastened and restrained from sliding or rotating.
3. Tighten the upper strap until the strap just barely makes contact with the sample wall, making sure not to over tighten the strap.

4. Hold the retaining device securely on the drill press table and begin drilling the hole slowly and in increments. Do not drill over half of the way through the sample, as cracking may occur.
5. Once the hole is drilled half of the way through the sample, release the straps and remove the sample from the retaining device.
6. Turn the sample over, now placing the end that was previously the bottom flush against the bottom side of the drilling template.
7. Tighten the lower strap and then proceed to lightly fasten the upper strap, making certain that you do not tighten over the point of the strap just touching the sample wall.
8. Hold the retaining device securely on the drill press table and proceed to drill through the remaining length of material.



Above: Picture of trial test samples using the new cutting and drilling procedures

Once a sample has been prepared from the raw FDOT boring it must undergo a 12-hour pre-spin in the rotating apparatus in order to remove any loose material that may have accumulated due to the boring, cutting, and drilling processes. The pre-spin procedure is described below.

Pre-Spin Procedure

1. Secure the guide plate in the top position on the slide-rail system.
2. Fill a polycarbonate insert 1/3 full with water.
3. Place the polycarbonate insert into the acrylic annulus.
4. Place a threaded rod in the sample and position it on the rod with the platens.
5. Gently attach the threaded rod to the guide plate and lower the sample into the test chamber. Tighten the guide plate in the correct position for testing.
6. Tighten the lid of the test chamber cylinder.
7. Fill the test chamber with water to the proper level.
8. Attach the constant rate water injection flow tube to the top of the test chamber.
9. Set the offset of the torque cell with the tare to 0.000 N-mm.
10. Turn on the motor and increase the RPM (displayed by a digital tachometer) until the desired torque of approximately 25 N-mm is achieved (displayed by a digital readout). Start the stopwatch.
11. Check to see if appropriate water level is maintained after spinning begins; use the water injection system to adjust the water level if necessary.
12. Allow the test to run for a minimum of 12 hours. Periodically check the ongoing test in order to adjust the motor speed for a constant torque on the sample and to

- ensure that the water level is maintained; set a flow rate for the water injection system if necessary.
13. After the minimum spin time, turn off the motor and allow the water within the annulus to cease motion. Record the duration of the experiment in minutes ($\Delta_{\text{pre-time}}$). Record the average torque in N-mm applied to the sample (T_{pre}).
 14. Undo the top screws of the lid and lift the guide plate up to where the sample is just out of the water. Secure the guide plate on the slide rail mechanism and let the residual water and eroded materials collect in the polycarbonate insert underneath the sample. Use the spray bottle to carefully wash the excess eroded material into the polycarbonate insert.
 15. Once the sample has ceased dripping and all the excess eroded material has been collected, lift and secure the guide plate in the top position on the slide-rail.
 16. Gently remove the threaded rod and sample from the guide plate.
 17. Gently remove the bottom platen and slide the sample off the threaded rod.
 18. Gently remove the polycarbonate insert containing the water and eroded material.

The sample is now ready for the pre-test laboratory experiments described in the next section. The machine should be cleaned after each experiment and prepared for the next test run.

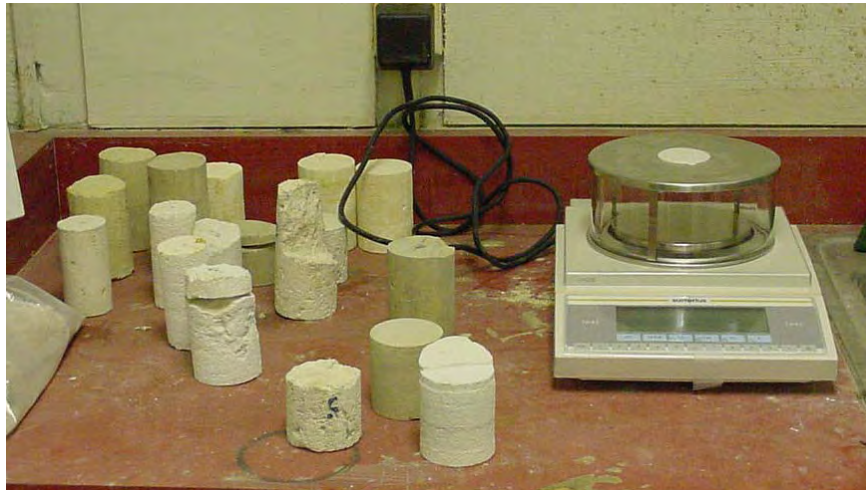
Obtaining Physical Properties of the Samples

Pre-test laboratory experiments are performed on the samples in order to obtain the physical properties of the specimen. The pre-test procedures are given below.

Procedures for Obtaining Physical Properties

1. Record the mass of the sample with the mass balance. ($m_{s\text{-pre-dry}}$)
2. Place the sample in the drying oven for at least 16 hours to dry. The sample is considered dry when the mass change is less than 0.1% in a period greater than one (1) hour. Record the final sample dry mass. ($m_{s\text{-pre-dry}}$)
3. Measure the diameter of the sample at a minimum of three (3) locations with the calipers and record the average diameter of the sample. (d_s)
4. Measure and record the length of the sample with the calipers. (l_s)
5. Fill the polycarbonate volumetric cylinder (heat resistant) of known mass and diameter ($m_{c\text{-pre}}$, D_c) with enough water to cover the top of the sample when immersed.
6. Mark the original water level with a dry-erase marker.
7. Gently immerse the dry sample in the water and immediately mark the wall of the cylinder where the new water level is located with a dry-erase marker.
8. Measure and record the change in height of the water levels. ($\Delta_{H_{20\text{-dry}}}$)
9. Wipe the water level marks off the cylinder.
10. Leave the sample submerged for a period of 16 hours, allowing the trapped air in the voids of the sample to escape.

11. After that time, lift the sample out of the water and allow the excess water to fall from the sample into the cylinder until the water ceases to drip.
12. Record the mass of the saturated sample. (m_{s-sat})
13. Mark the water level in the cylinder with a dry-erase marker.
14. Gently immerse the saturated sample in the water, start the stopwatch, and immediately mark the wall of the cylinder with a dry-erase marker where the new water level is located.
15. Measure the change in height of the water level and record this value. (Δ_{H_2O-sat})
16. Leave the sample submerged in the cylinder with the same water and eroded material until ready to test. The sample is kept hydrated in order to simulate a saturated rock formation as may be found in the bed of a natural waterway.



Above: Picture of trial samples and digital mass scale



Above: Picture of lab area and test equipment

Erosion Rate Testing Procedures

1. Secure the guide plate in the top position on the slide-rail system.
2. Lift the immersed sample out of the water and allow the excess water to fall from the sample into the volumetric cylinder until the water ceases to drip.
3. Place a threaded rod in the sample and position it on the rod with the platens.
4. Gently attach the threaded rod to the guide plate.
5. Place the polycarbonate volumetric cylinder with the water and eroded material in the drying oven for at least 16 hours, noting the volumetric cylinder's ID number. The volumetric cylinder and eroded material are considered dry when the mass change is less than 0.1% in a period greater than one (1) hour. Record the dry mass of the volumetric cylinder and eroded material. ($m_{c\text{-post-dry}}$)

6. Fill a polycarbonate insert of known mass ($m_{\text{insert-pre}}$) 1/3 full with water. (It is important to note that water from the actual field site where the sample was collected should be used)
7. Place the polycarbonate insert into the acrylic annulus.
8. Measure and record the temperature of the water. ($\text{Temp}_{\text{H}_2\text{O-pre}}$)
9. Gently lower the sample into the test chamber. Tighten the guide plate in the correct position for testing.
10. Tighten the lid of the test chamber cylinder.
11. Fill the test chamber with water to the proper level.
12. Attach the constant rate water injection flow tube to the top of the test chamber.
13. Set the offset of the torque cell with the tare to 0.000 N-mm.
14. Turn on the motor and increase the RPM (displayed by a digital tachometer) until the desired torque is achieved (displayed by a digital readout). Start the stopwatch.
15. Check to see if appropriate water level is maintained after spinning begins; use the water injection system to adjust the water level if necessary.
16. Allow the test to run for a minimum of 72 hours. Periodically check the ongoing test in order to adjust the motor speed for a constant torque on the sample and to ensure that the water level is maintained; set a flowrate for the water injection system if necessary.
17. After the minimum spin time, turn off the motor and allow the water within the annulus to cease motion. Record the duration of the experiment in minutes (Δ_{time}). Record the average torque in N-mm applied to the sample (T).

18. Remove the top screws of the lid and lift the guide plate up to where the sample is just barely out of the water. Secure the guide plate on the slide rail mechanism and let the residual water and eroded materials collect in the polycarbonate insert underneath the sample. Use the spray bottle to carefully wash the excess eroded material into the polycarbonate insert.
19. Once the sample has ceased dripping and all the excess eroded material has been collected, lift and secure the guide plate in the top position on the slide-rail.
20. Measure and record the temperature of the water. ($\text{Temp}_{\text{H}_2\text{O-post}}$)
21. Gently remove the polycarbonate insert containing the water and eroded material.
22. Place the polycarbonate insert into the oven and record the insert ID number. Leave in the drying oven for at least 16 hours. The insert and material are considered dry when the mass change is less than 0.1% in a period greater than one (1) hour. Record the dry mass of the insert and eroded material. ($m_{\text{insert-post}}$)
23. If another erosion test is to be performed immediately on this sample then repeat steps 6 – 22. If the testing sequence is done then gently remove the threaded rod and sample from the guide plate.
24. Gently remove the bottom platen and slide the sample off the threaded rod.
25. Place the sample into the oven. Leave in the drying oven for at least 16 hours. The sample is considered dry when the mass change is less than 0.1% in a period greater than one (1) hour. Record the dry mass of the sample. ($m_{\text{s-post-dry}}$)

Calculations from above procedures

A master spreadsheet has been developed that will accept the data from the above procedures. No initial calculations are necessary, the corresponding physical properties and rate of erosion will be calculated by inputting all of the noted values. The calculations of the physical properties as well as the rate of erosion are outlined below.

Calculations for Physical Properties

1. Calculate the surface area of the sample (A_s)

$$A_s = \pi * d_s * l_s$$

2. Calculate the amount of material lost in the saturation process (m_{lost}).

$$m_{lost} = m_{c-post-dry} - m_{c-pre-dry}$$

3. Calculate the adjusted dry mass of the sample ($m_{s-dry-adj}$).

$$m_{s-dry-adj} = m_{s-pre-dry} - m_{lost}$$

4. Calculate the absorbed mass ($m_{absorbed}$).

$$m_{absorbed} = m_{s-sat} - m_{s-dry-adj}$$

5. Calculate the volume of water displaced by the dry sample (V_{dry}).

$$V_{dry} = (\Delta_{H_2O-dry}) * (0.25 * \pi * D_c^2)$$

6. Calculate the volume of water displaced by the saturated sample (V_{sat}).

$$V_{sat} = (\Delta_{H_2O-sat}) * (0.25 * \pi * D_c^2)$$

7. Calculate the dry density of the sample (ρ_{dry}).

$$\rho_{dry} = m_{s-dry-adj} / V_{dry}$$

8. Calculate the wet density of the sample (ρ_{sat}).

$$\rho_{sat} = m_{s-sat} / V_{sat}$$

Calculations for Rate of Erosion

1. Calculate the mass of the eroded material (m_{erosion}).

$$m_{\text{erosion}} = m_{\text{insert-post}} - m_{\text{insert-pre}}$$

2. Calculate the shear stress on the sample (τ).

$$\tau = T / (d_s/2) / A_s$$

3. Calculate the erosion rate (e).

$$e = m_{\text{erosion}} / \rho_{\text{dry}} / A_s / \Delta_{\text{time}}$$

4. Calculate the total mass lost do to erosion ($m_{\text{eroded-total-1}}$).

$$m_{\text{eroded-total-1}} = m_{\text{s-dry-adj}} - m_{\text{s-post-dry}}$$

5. Calculate the total mass lost due to erosion from all the test trials ($m_{\text{eroded-total-2}}$).

$$m_{\text{eroded-total-2}} = \sum m_{\text{erosion}}$$

6. Calculate the difference between the two total eroded mass values (Δ_m).

$$\Delta_m = m_{\text{eroded-total-1}} - m_{\text{eroded-total-2}}$$

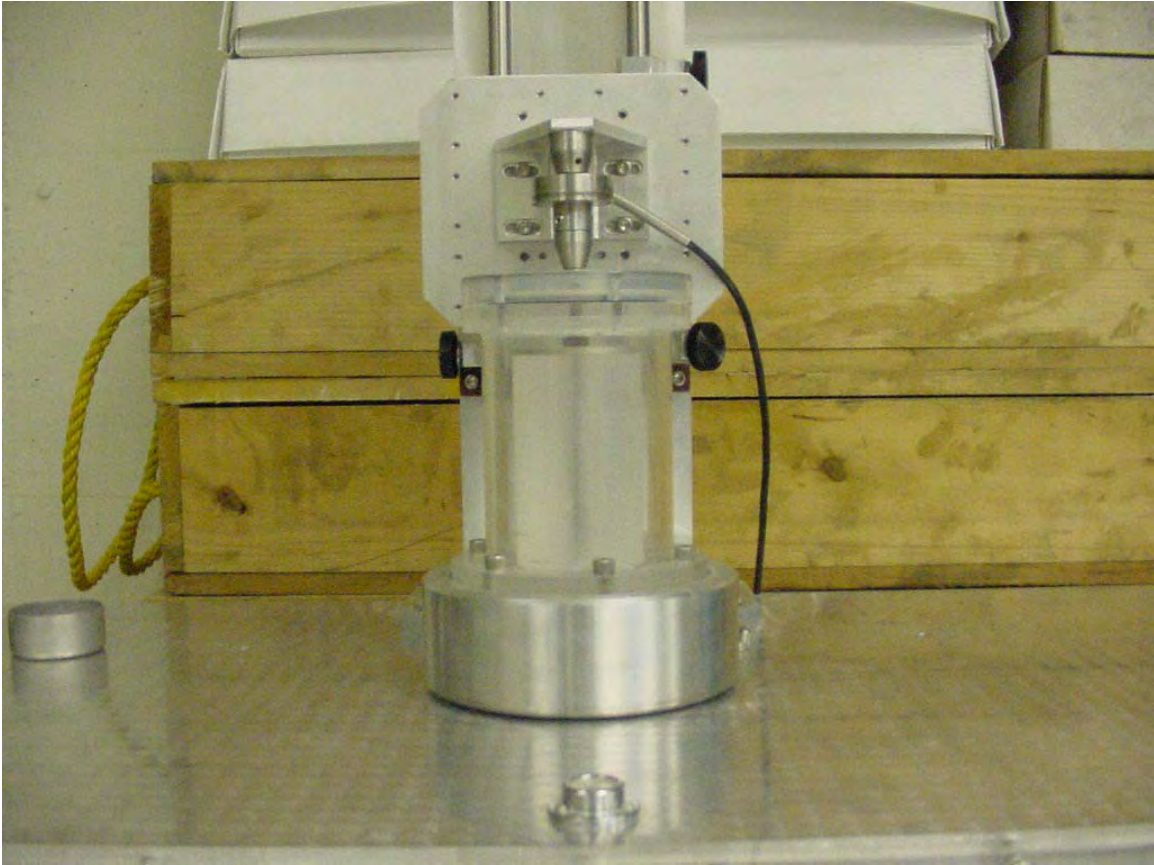
7. Calculate the change in temperature (Δ_{temp}).

$$\Delta_{\text{temp}} = \text{Temp}_{\text{H}_2\text{O-post}} - \text{Temp}_{\text{H}_2\text{O-pre}}$$

RETA PHOTOGRAPHS



Rotating Erosion Test Apparatus (RETA)



RETA Acrylic Cylinder and Torque Cell



RETA Sample Slide Rail

RETA TEST RESULTS

Specimen Information

FDOT Core Information

Project	Chipola River Bridge on I-10			
	UF Sample #			
	1	2	3	4
Type	Design	Design	Design	Design
Bridge	Br 53	Br 52	Br 53	Br 52
Core ID	S 4-5	S 2-4	S 3-3	S 1-2
Elevation	52' NGVD	50' NGVD	49' NGVD	41' NGVD
Description	Tan Brown Limestone			

FDOT Test Results

	UF Sample #			
	1	2	3	4
Uniaxial Compressive Strength ()				
Tensile Strength ()				
L.A. Abrasion Test ()				
Sulfate Soundness Test ()				

Pre-Test Spin Information

	UF Sample #			
	1	2	3	4
RPM	1500	1500	1500	1500
Torque (N-mm)	5.2	5.4	5.4	5.2
Duration (min)	1560	1545	1442	1441

Specimen Preparation Data Sheet

Dimensions

	UF Sample #			
	1	2	3	4
Length (cm)	9.67	9.77	9.27	8.37
Diameter (cm)	6.09	6.09	6.08	6.10
Surface Area (cm ²)	185.01	186.92	177.07	160.40

Lab Analysis Data

Dry Specimen

Original Dry Mass (g)	593.520	527.858	535.650	500.256
Final Dry Mass (g)	593.460	527.845	535.623	500.243
ΔH Dry Sample (cm)	1.89	1.75	1.68	1.62
Cylinder Radius (cm)	6.90	6.90	6.90	6.90
Volume of Dry Sample (cm ³)	282.69	261.75	251.28	242.31
Density of Dry Sample (g/cm ³)	2.10	2.02	2.13	2.06

Absorption

Initial Mass Container + Water (g)	1753.26	1725.36	1782.65	1761.33
Final Mass Container + Water (g)	1751.39	1723.95	1781.15	1759.89
Time of Absorption (sec)	45	56	52	49
Absorption (g)	1.87	1.41	1.50	1.44

Polycarbonate Inserts

	Trial #		
	1	2	3
Initial Insert Dry Mass (g)	74.565	74.602	74.611
	74.567	74.607	74.616
	74.577	74.612	74.603
	74.522	74.602	74.598

Erosion Rate Testing Data

UF Sample #	1
-------------	---

	Trial		
	1	2	3
Initial Insert Dry Mass (g)	74.565	74.602	74.611
Initial Water Temp. (°C)	23.5	23.9	24.2
Measured Spinrate (RPM)	2000	3000	4000
Measured Torque (N-mm)	8.9	21.9	36.5
Calculated Stress (Pa)	15.8	38.9	64.8
Temp. (°C)	24.6	25.3	25.8
Final Insert Dry Mass (g)	74.665	74.803	74.926
Test Duration (min)	4440.5	5456	4512
Specimen Mass Lost (g)	0.100	0.201	0.315
Δ Water Temp (°C)	1.1	1.4	1.6
Converted Stress (lb/ft ²)	0.33	0.82	1.36
Erosion Rate (in/hr)	1.37E-06	2.24E-06	4.25E-06
Erosion Rate (in/month)	9.86E-04	1.61E-03	3.06E-03
Erosion Rate (in/year)	1.20E-02	1.96E-02	3.72E-02

Duration			
(hrs)	74	90	75
(min)	0.5	56	12
Calculated Stress (Pa)	15.8	38.9	64.8

Erosion Rate			
(mm/hr)	3.48E-05	5.69E-05	1.08E-04
(mm/month)	2.50E-02	4.10E-02	7.77E-02
(cm/year)	3.05E-02	4.99E-02	9.45E-02

UF Sample #	2
-------------	---

	Trial		
	1	2	3
Initial Insert Dry Mass (g)	74.567	74.607	74.616
Initial Water Temp. (°C)	22.9	24	23.5
Measured Spinrate (RPM)	2000	3000	4000
Measured Torque (N-mm)	7.9	19.6	38.2
Calculated Stress (Pa)	13.9	34.4	67.1
Temp. (°C)	23.5	24.9	25.2
Final Insert Dry Mass (g)	74.645	74.753	74.863
Test Duration (min)	4476	4526	4485
Specimen Mass Lost (g)	0.078	0.146	0.247
Δ Water Temp (°C)	0.6	0.9	1.7
Converted Stress (lb/ft ²)	0.29	0.72	1.41
Erosion Rate (in/hr)	1.09E-06	2.02E-06	3.45E-06
Erosion Rate (in/month)	7.86E-04	1.46E-03	2.48E-03
Erosion Rate (in/year)	9.57E-03	1.77E-02	3.02E-02

Duration			
(hrs)	74	75	74
(min)	36	26	45
Calculated Stress (Pa)	13.9	34.4	67.1

Erosion Rate			
(mm/hr)	2.77E-05	5.13E-05	8.77E-05
(mm/month)	2.00E-02	3.70E-02	6.31E-02
(cm/year)	2.43E-02	4.50E-02	7.68E-02

UF Sample #	3
-------------	---

	Trial		
	1	2	3
Initial Insert Dry Mass (g)	74.577	74.612	74.603
Initial Water Temp. (°C)	22.5	23.2	22.7
Measured Spinrate (RPM)	2000	3000	4000
Measured Torque (N-mm)	8.2	17.6	36.9
Calculated Stress (Pa)	15.2	32.7	68.6
Temp. (°C)	23.2	24.1	23.9
Final Insert Dry Mass (g)	74.646	74.773	74.885
Test Duration (min)	4436	4390	4325
Specimen Mass Lost (g)	0.069	0.161	0.282
Δ Water Temp (°C)	0.7	0.9	1.2
Converted Stress (lb/ft ²)	0.32	0.69	1.44
Erosion Rate (in/hr)	9.74E-07	7.01E-04	8.53E-03
Erosion Rate (in/month)	2.30E-06	1.65E-03	2.01E-02
Erosion Rate (in/year)	4.08E-06	2.94E-03	3.57E-02

Duration			
(hrs)	74	73	72
(min)	26	10	5
Calculated Stress (Pa)	15.2	32.7	68.6

Erosion Rate			
(mm/hr)	2.47E-05	5.83E-05	1.04E-04
(mm/month)	1.78E-02	4.20E-02	7.46E-02
(cm/year)	2.17E-02	5.11E-02	9.08E-02

UF Sample #	4
-------------	---

	Trial		
	1	2	3
Initial Insert Dry Mass (g)	74.522	74.602	74.598
Initial Water Temp. (°C)	22.9	23.2	23.4
Measured Spinrate (RPM)	2000	3000	4000
Measured Torque (N-mm)	8.9	21.9	36.5
Calculated Stress (Pa)	18.2	44.8	74.6
Temp. (°C)	23.4	24.2	24.8
Final Insert Dry Mass (g)	74.672	74.813	74.935
Test Duration (min)	4330	4335	4385
Specimen Mass Lost (g)	0.15	0.211	0.337
Δ Water Temp (°C)	0.5	1.0	1.4
Converted Stress (lb/ft ²)	0.38	0.94	1.57
Erosion Rate (in/hr)	2.47E-06	3.47E-06	5.48E-06
Erosion Rate (in/month)	1.78E-03	2.50E-03	3.95E-03
Erosion Rate (in/year)	2.16E-02	3.04E-02	4.80E-02

Duration			
(hrs)	72	72	73
(min)	10	15	5
Calculated Stress (Pa)	18.2	44.8	74.6

Erosion Rate			
(mm/hr)	6.28E-05	8.82E-05	1.39E-04
(mm/month)	4.52E-02	6.35E-02	1.00E-01
(cm/year)	5.50E-02	7.73E-02	1.22E-01